Benthic foraminifera and pore water carbonate chemistry on a tidal flat and salt marsh at Ria Formosa, Algarve, Portugal

Joachim Schönfeld [a, *] and Isabel Mendes [b]

[a] GEOMAR Helmholtz Zentrum für Ozeanfoschung Kiel, Wischhofstrasse 1-3, 24148, Kiel, Germany.
[b] Centro de Investigação Marinha e Ambiental (CIMA), Universidade do Algarve, Campus de Gambelas, 8005-139, Faro, Portugal.
[*] Corresponding author. E-mail address: jschoenfeld@geomar.de (J. Schönfeld).

Abstract

Benthic foraminifera showed a vertical zonation in tidally influenced salt marshes, which has been used for sea level reconstructions. Growing evidence suggested that freshwater influx, salinity, or the pH of interstitial waters has also an impact on the foraminiferal distribution. A tidal flat and salt marsh transect was investigated in the north-western Ria Formosa coastal lagoon, Algarve, Portugal, to constrain the relationship of benthic foraminifera, halophytes, and pore water properties. The dominance of saltworts from the subfamily Salicornioideae and landward increasing soil salinities depicted evaporation as governing environmental factor. The carbonate chemistry from lagoonal and pore waters identified anoxic tidal flat sediments of as main source of total alkalinity. The alkalinity was lower in the salt marsh, where the pCO_2 was extremely high. Salt marsh pore waters showed a high variability of carbonate system parameters, which mirrored small-scale spatial heterogeneities in the soil. The distribution of textulariid salt marsh foraminifera was confined to the vegetated zones, where their abundance increased with elevation. Calcareous species were frequent on the tidal flat and in the highest salt marsh. Many of them were specialised to high salinities or to extreme and variable environmental conditions. Two levels of faunal change in the salt marsh coincide with vegetation zonal boundaries, mean tide or mean high water levels. The two other faunal changes were related to changes in calcite saturation state or organic carbon concentrations. The proportion of textulariids showed a negative correlation with submergence time or elevation, and a significant correlation with pore water pCO_2. The faunal distribution, pore water calcite saturation, and *Ammonia* dissolution patterns indicated that calcareous species specialised to tolerate carbonate-corrosive conditions prevailed even at lowest saturation levels.

Keywords: Ria Formosa, Intertidal, Salt marsh, Foraminifera, Salinity, Carbonate chemistry

1. Introduction

Living benthic foraminifera were found in marginal marine environments up to the highest reach of marine floodings (Lehmann, 2000; Müller-Navarra et al., 2017). In particular the salt marshes above mean high water level are inhabited by an unique fauna of agglutinated species (Phleger, 1970; Camacho et al., 2015a). This fauna comprises a few tens of cosmopolitan taxa (Murray, 1971). Their diversity declines with geographical latitude and elevation in the tidal frame (Lübbers and Schönfeld, 2018). A coincidence of species distribution ranges with the marsh vegetation zones was recognised (Phleger, 1965a; Lutze, 1968). These observations lead to the assumption that the species were adapted to distinct halophytic plants (Scott, 1976). Later studies revealed the same foraminiferal zonations prevailing in different climatic zones and floral biogeographic regions (Scott and Medioli, 1978).

Hydrographical surveys, instrumental monitoring, and laboratory experiments demonstrated that marginal marine foraminifera may tolerate a high range and variability of ambient temperature, salinity, pH and oxygen concentrations (Bradshaw, 1961, 1968). Instead, the inundation frequency, desiccation, and the influence of precipitation or freshwater influx were constrained as factors governing the distribution of salt marsh foraminifera (Hayward et al., 2004; Horton and Murray, 2007). The inundation frequency co-varies with elevation in tidally influenced marshes (Cearreta et al., 2002; Fatela et al., 2013; Francescangeli et al., 2017; Mueller-Navarra et al., 2017). Salt marsh foraminifera have therefore been extensively applied as sea level proxies (Scott and Medioli, 1978, 1980; Gehrels, 1994; Hayward et al., 1999, Horton et al., 1999; Gehrels et al., 2001, 2006; Edwards et al., 2004; Horton and Edwards, 2006; Barnett et al., 2016). Other studies found salinity variations having more

influence on the observed foraminiferal distributional patterns than elevation (De Rijk, 1995; de Rijk and Troelstra, 1997; Moreno et al., 2012).

The predominance of agglutinated species in salt marsh foraminiferal faunas was first explained by the low pH of salt marsh soils, which may dissolve the tests or inhibit the shell formation of calcareous species (Parker and Athearn, 1959; Phleger, 1965b, 1970). Humic acids of salt marsh peat or surface runoff from catchment areas with acetic soils compensated or outbalanced the influence of alkaline sea water (Moreno et al., 2007; Fatela et al., 2009; Korsun et al., 2014). Rain and CO_2 produced by microbial decay of plant debris was also suggested to depress the pH of interstitial waters in the marshes (e.g. Reaves, 1986; Lübbers and Schönfeld, 2018).

Iberian estuaries provided a more detailed picture. For instance, calcareous species were living in vegetated marshes at and above mean high water level in the Plentzia Estuary, northern Spain, where the sediment contains limestone debris (Cearreta and Murray, 2000; Cearreta et al., 2002). In the normal saline Lima Estuary, northern Portugal, calcareous foraminifera were abundant in low marsh samples at pore water pH values of 7.1. They were on average 1 unit higher than in the marsh soil of the adjacent low-saline Minho/Coura Estuary, where only agglutinated species prevailed (Moreno et al., 2005, 2007; Valente et al., 2009). The salt marsh pore water alkalinity was on average same as high as in estuarine waters of Minho/Coura Estuary and calcite undersaturated. In Lima salt marsh, the pore water alkalinity was 4.8 fold higher than in the estuary and the calcite saturation index suggests almost equilibrium conditions (Valente et al., 2009).

Experimental studies revealed that tests of many near-shore calcareous foraminiferal species were corroded at calcite-undersaturated conditions while they survive (e.g. LeCadre et al., 2003; Haynert et al., 2011; Haynert and Schönfeld, 2014; Saraswat et al., 2015). Some specimens were able to recalcify their tests though at higher energetic costs and with thinner shells than at saturated conditions (Alison et al., 2010; Melzner et al., 2011; Haynert et al., 2014). Other species were not affected (Vogel and Uthicke, 2012; McIntyre-Wressing et al., 2013). It has been proposed that pore waters enriched in alkalinity by remineralisation products from the decay of organic matter may facilitate the survival of endobenthic calcareous foraminifera under carbonate corrosive conditions and elevated pCO_2 levels (Thomas et al., 2009; Haynert et al., 2014; Amergian et al., 2022).

The purpose of the present paper is to better constrain the relationship of benthic foraminifera and pore water properties in intertidal environments. The above mentioned hypothesis was further specified: pore water carbonate system parameters are exerting a governing influence on the distribution of foraminiferal species in salt marshes rather than salinity or inundation frequency in the tidal frame. A salt marsh transect in the north-western Ria Formosa coastal lagoon was investigated to test this hypothesis. The living foraminiferal faunas were compared to halophyte associations, elevation in the tidal frame, and hydrographic properties as salinity, pH, alkalinity, pCO_2. and calcite saturation of interstitial waters from their habitat.

1.1. Geographical and environmental setting

Ria Formosa coastal lagoon has a surface area of 105 km^2. It is protected from the adjacent ocean by a chain of five barrier islands and two peninsular spit bars. Six broad inlets effect a complete water exchange with the Gulf of Cadiz during each tidal cycle (e.g. Tett et al., 2003; Pacheco et al., 2010; Rosa et al., 2019). The intertidal area of the lagoon is dominated by sand or mud flats, and extended salt marshes. They are intersected by a complex network of channels and tributaries (Fig. 1), of which Esteiro do Ancão serves the north-western part of Ria Formosa (Andrade et al., 2004). The tidal flats pass into extended salt marshes, which gather around small elongated sand ridges of supratidal height (Carrasco et al., 2021). These sand ridges are detached from the mainland and represent ancient flood deltas that were formed by barrier breaching during extreme storm events (Andrade et al., 2004).

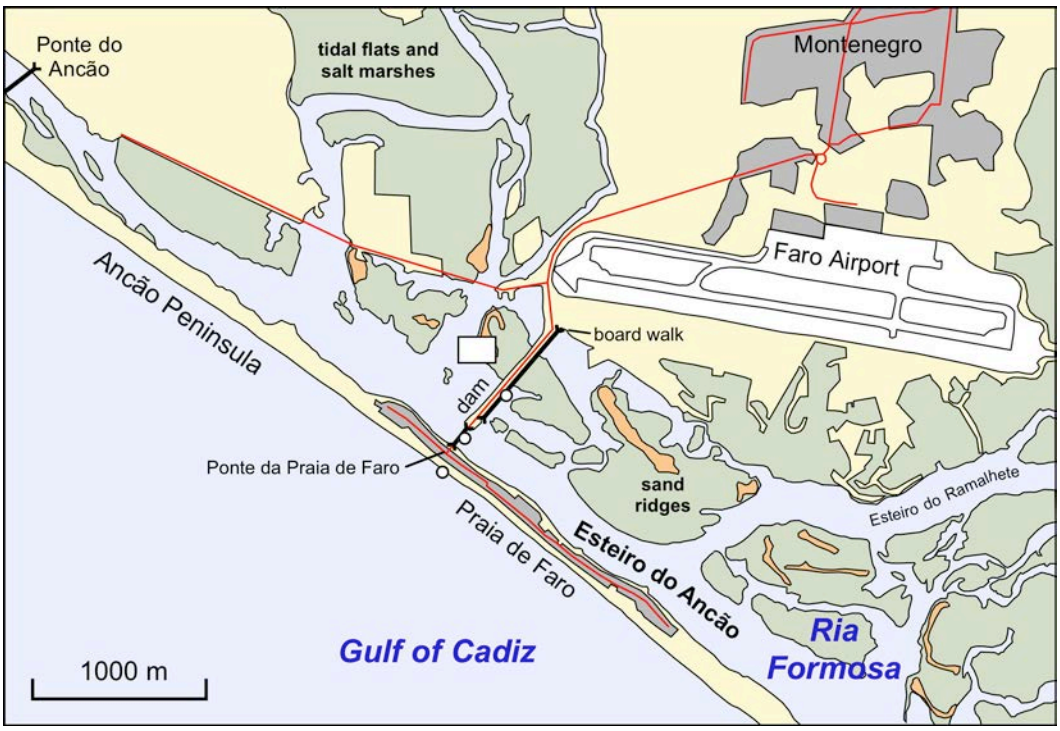

Fig. 1. Geography of the study area. Grey: urban areas, red lines: main roads, square: investigation site (Fig. 2), circles: sampling sites for hydrographical measurements and tide gauge. Redrawn after Carta Militar de Portugal, Folha 610, 611, © Instituto Geográfico do Exército, Lisboa, 2006.

The salt marshes of the north-western Ria Formosa are disconnected by a dam and the bridge to Praia de Faro crossing Esteiro do Ancão (Fig. 1). Salinities and water temperatures measured at the bridge during short-term hydrographic surveys ranged from 34.4 to 37.1 units and 17.0 to 25.7°C in April to May 2013 through 2019 (Schönfeld and Mendes, 2021). Long-term data sets showed ranges from 15 to 39 salinity units and 9 to 30°C in the western part of the lagoon (Barbosa, 2010). The average amplitude of semidiurnal spring-tides is 2.8 m, the average neap-tide amplitude is 1.3 m (Pacheco et al., 2010). The mean tidal level at the bridge was constrained to 0.34 m with reference to the Portuguese Ordnance Datum (POD) (Schönfeld and Mendes, 2021). The geodetic reference of POD (zero cartográfico) is the mean sea level at Cascais recorded from 1882 to 1938 (nível médio adotado) (Alves da Silva et al., 2008).

Intertidal floral associations in the north-western part of Ria Formosa commence with dense meadows of sea grass (*Zostera noltii*) on levee-shaped mud banks or tidal flats alongside small channels and tributaries (e.g. Carrasco and Matias, 2019). Green macroalgae (*Enteromorpha* sp., *Ulva* sp.) grow on sand flats. They may develop a dense cover in places, in particular during autumn and winter (Aníbal, 2019).
The saltmarsh flora of Ria Formosa is associated with other southwest Portuguese Atlantic salt marshes south of Tagus River estuary. They are characterised by both, Atlantic and Mediterranean halophytes (Costa et al., 2009). The pioneer zone is vegetated by the salt marsh grass *Spartina maritima* and *Spartina densiflora*, the lower and upper salt marsh by different saltwort taxa of the subfamily Salicornioideae, as well as *Halimione portulacoides, Juncus* spp., and *Limoniastrum monopetalum* (e.g. Costa et al., 1996; Muzavor et al., 2010; de los Santos et al., 2022).

1.2. Foraminiferal assemblages

Benthic foraminifera were scarcely investigated at Ria Formosa to date. Thirty-seven foraminiferal species or groups were recorded in surface sediment samples from western Ria Formosa channels (Andrade et al., 2004). Living, i.e. rose-Bengal stained specimens were very rare. Among intertidal species, *Ammonia tepida* was abundant in the living fauna and *Haynesina germanica* was frequent in the dead assemblage. A monitoring study in the intertidal zone of Esteiro do Ancão backbarrier beach reported 105 foraminiferal species living in medium to coarse sands with pebbles and shell debris, and in sandy to clayey muds close to the main channel (Schönfeld and Mendes, 2021). The majority of the species were known from subtidal, continental shelf and fjord environments of the northern

Atlantic and marginal seas. Salt marsh or intertidal species were rare. In the sands around and above mean high water level, *Entzia macrescens, Trochammina inflata*, other trochamminids, and most importantly, a considerable number of large, robust specimens of the calcareous species *Rosalina globularis* were found (Schönfeld and Mendes, 2021).

1.3. Hydrochemistry and carbonate system parameters

The inventory of nutrients and trace metals, their spatial and temporal variability in Ria Formosa lagoonal waters are well known (e.g. Falcão and Vale, 1990; Asmus et al., 2000; Newton and Mudge, 2005; Loureiro et al., 2006; Brito et al., 2010; Domingues et al., 2017). The nutrient concentrations in lagoonal waters are usually higher than in the adjacent ocean due to benthic remineralisation processes, and, with the exception of nitrate during coastal upwelling events, a net export of nutrients takes place during each tidal cycle (Cravo and Jacob, 2019).

Total alkalinity (TA) and surface ocean CO_2 pressure (pCO_2) may be variable in near-coastal waters of the northern Atlantic, due to blooms of calcifying planktonic organisms, coastal upwelling and the influx of rivers (Rost and Riebesell, 2004; Cabeçadas and Oliveira, 2005; Cai et al., 2010). Estuarine systems export dissolved inorganic carbon (DIC) and TA to the adjacent ocean (e.g. Ribas-Ribas et al., 2013; Wang et al., 2016; Oliveira et al., 2017). Particularly, the export from Rio San Pedro, Spain, to the Gulf of Cadiz was found to be determined by the seasonal varying input from marshes, fish farm production, and the seasonality of phytoplankton (de la Paz et al., 2008). Only a few TA measurements were made at Ria Formosa to date (Range et al., 2011; 2012). The reported average values of 3252 and 3583 µmol kg^{-1} were 340 to 680 µmol kg^{-1} higher than in Rio San Pedro estuary, and 810 to 1140 µmol kg^{-1} higher than in the Gulf of Cadiz (2440 µmol kg^{-1}; de la Paz et al., 2007).

2. Material and methods

The field work for the present study has been performed in combination with sampling for the foraminiferal time series at Esteiro do Ancão in April to May 2013 through 2019 (Schönfeld and Mendes, 2021). The investigations reported herein are based on samples, observations and measurements taken during the campaigns in 2018 and 2019. We concentrated on the salt marsh immediately to the North of the dam with the road to Praia de Faro (Fig. 1). The study area is situated west of a 2 m high, supratidal sand ridge, which is accessible from the road to Praia de Faro via an abandoned foot path. A 94-m long East-West transect was defined, commencing at the spring high-water line above the foot path at 37°0.809'N and 7°59.545'W, heading to 263° (WSW) up to a concrete post in the middle of a mud flat 4 m beyond a small tidal channel (Fig. 2). The surface height was determined with a Leica NA728 surveyor's level at 1 – 3 m intervals along the transect. The levels were related to a local reference point on the sand ridge (2.067 m POD), which was tied to the geodetic reference points IHBH 29/99 at the bus turn on the dam (2.660 m POD), and the reference point DGP MBH4 on the bridge platform (3.291 m POD). The accuracy was 0.006 and 0.008 m when linking the local and geodetic reference points forth and back respectively, over a distance of 1230 m.

Sediment composition, surface structures, halophyte and macrophyte occurrences, and macroorganism were inspected and described along the transect. The examinations were performed by two persons in order to assess the boundaries between halophyte associations with more certainty. We distinguished the upper and lower saltmarsh, and the pioneer zone following Suchrow (2014). The plants were identified by using the illustrated guide of Muzavor et al. (2010) and online resources (e.g. https://flora-on.pt/).

Foraminiferal samples were taken along the transect at distances of 2 – 11 m. The sample positions were chosen according to halophyte associations and sedimentary structures. The positions were tagged with plant nursery labels in gaps or under the vegetation, which facilitated a retrieval of the same spot in the following year. A chamfered stainless steel tube of 35 mm inner diameter and 10 cm^2 void area, a graduated plastic ring of the same diameter, and a shuffle spatula was used to detach the uppermost 1 cm of the sediment on the tidal flats (Schönfeld et al., 2012). In the salt marsh, the sharp steel tube was pierced through the root-bound top soil and turned. The device was dug out, the core inside was pushed up, and the top 1 cm was cut off with a kitchen knife. Shell fragments or roots often obstructed the sample detachment leading to volumes that were higher or lower than 10 cm^3. The samples were transferred into 100 mL PVC (Kautex®) bottles, preserved and

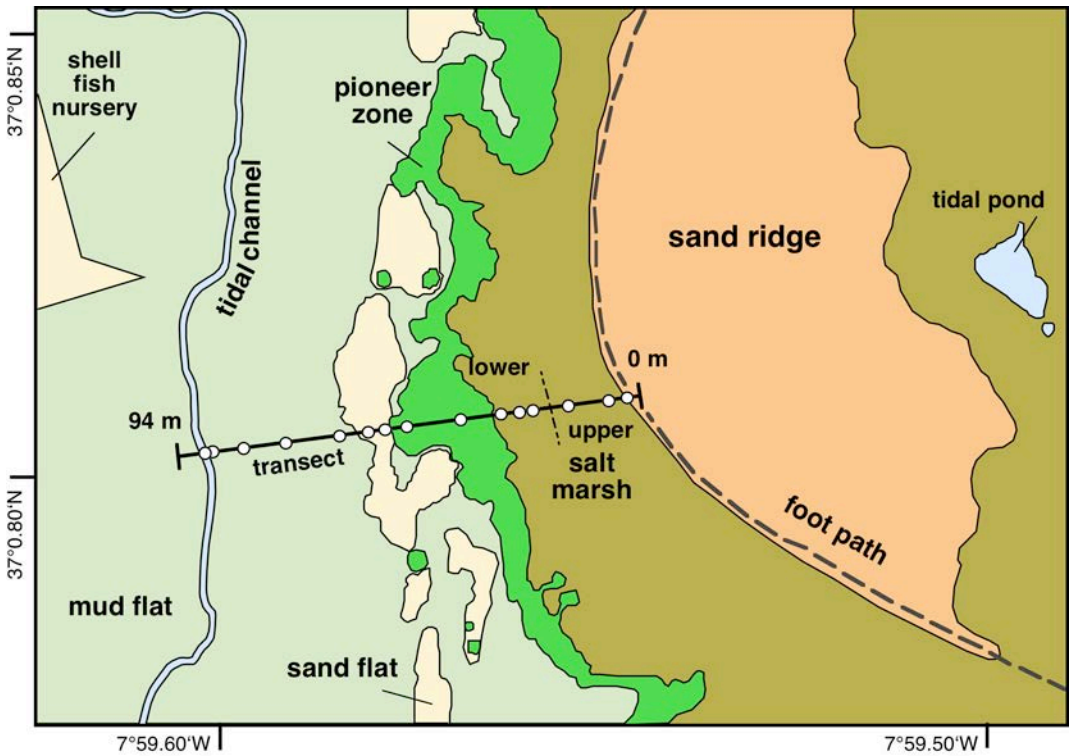

Fig. 2. Location map of the investigated transect in the north-western Ria Formosa salt marsh. Circles: sampling sites. The floral zones and sedimentary units were identified by personal observations. The map was drawn after areal photographs and satellite images.

stained with a rose Bengal solution of 2 g in 1 l vodka (40 %) for shipment as non-dangerous substance (Schönfeld, 2012). The ethanol concentration was raised to >90 % after transport for long-term storage (Schönfeld and Mendes, 2021). The foraminiferal sampling techniques applied herein differed from the FOBIMO recommendations but have been proven appropriate for explorative studies in salt marshes (Lübbers and Schönfeld, 2018).

The foraminiferal samples were analysed following the methods and procedures described by Schönfeld and Mendes (2021). In brief, the samples were gently washed with carbonate-saturated tap water through stacked sieves of 63 and 2000 µm mesh size. Well-stained foraminifera that were living at the time of sampling were picked wet from the 63-2000 µm size fraction. The sample residues or aliquots were picked completely. Aliquots were made with a Motodo wet splitter only when the total number of individuals was expected to exceed ca. 300 specimens. The individuals were collected in Plummer cell slides, sorted by species, fixed with glue, and counted. The test preservation of *Ammonia* spp. was assessed separately referring to the classifications of Le Cadre et al (2003) and Haynert et al (2011). The following preservation stages were defined in this study: 1 = intact, glossy test, 2 = dull shell wall, 3 = dissolution or loss of the last chamber, 4 = dissolution of more chambers with the inner organic lining visible, 5 = almost complete dissolution of the outer chamber wall, star-shape test (Supplement Fig. 1). The *Ammonia* dissolution index was calculated as weighed mean from the individual number of specimens affiliated with a particular preservation stage. Images for species' documentation were taken with a Keyence VHX-7000 digital microscope at the Institute of Geosciences, Kiel University. The Fisher alpha diversity indices were calculated with Past v3.16 (Hammer et al., 2001).

Additional surface sediment samples were taken for total organic carbon (Corg) analyses at the foraminifera sampling sites by using 10-cm^3 cut-off syringes of 1.5 cm diameter. The syringes were capped after sampling, stored and transported at cool conditions in plastic bags with a water-saturated atmosphere. In the laboratory, a defined volume of 9 to 10 cm^3 was freeze-dried and ground with a ball mill or an agate mortar before further analyses. The Corg content was determined with a Carlo Erba Elemental Analyzer by using standard methods (https://www.geomar.de/en/research/fb2/fb2-mg/benthic-biogeochemistry/mg-analytik/determination-of-cns).

A hydrographic monitoring station was installed under the board walk at 37°0.683'N and 7°59.467'W to assess the long-term mean high water levels, and the seasonal variability of air and water temperature, and high water salinity (Fig. 1). The measurements were taken at 20-minutes intervals with two Odyssey pressure–temperature and two conductivity-temperature recorders, and one EBI-20T air temperature data logger from 08-May-2019 to 12-July-2020 and 22-August-2020 (EBI-20T only). They were serviced on 29-November-2019. The heights of the Odyssey pressure and conductivity sensors were tied to the geodetic reference point DGP MBH4 on the bridge. The sensor accuracy was ±0.5 cm for immersion, ±0.23 K for temperature, and ±0.18 salinity units after calibration with standard solutions (1-sigma values; Schönfeld, 2018). The external reproducibility was +0.3/-2.7 cm, on average 1.4 cm (n = 11), as depicted by a comparison of logger records and on-site measurements with a folding rule. The accuracy of EBI-20T temperature sensor is ±0.1 K. Mean water temperatures and salinities were calculated from the recordings at high water times. One Odyssey pressure–temperature logger failed after the maintenance in November 2019. Therefore, the record of the other logger was used for the entire period. Mean high water levels were calculated over one lunar year of 354 days from New Moon on 3-June-2019 (Lunation 1193) to New Moon on 22-May-2020 (Lunation 1205). The four highest high waters around Full or New Moon were considered as spring tides, while the four lowest high waters around the First or Last Quarter were considered as neap tides. The lunar phases were taken from online resources (e.g. https://timeanddate.de). The inundation time for levels above the sensor of the pressure-temperature logger (0.61 m POD) was calculated from all measurements during the above lunar year by using the histogram function of Microsoft® Excel®. The inundation frequency is expressed as percent submergence time of the one lunar year observation period.

Hydrographic investigations also include sampling of shallow water above the immersed pioneer vegetation zone and in the tidal channel at the salt marsh transect investigated, ebb waters of Esteiro do Ancão taken at the bridge (main conduit, navigation channel), and surface water from the Gulf of Cadiz taken at Praia de Faro (Fig. 1). A 1.0 L polypropylene pitcher and a polyester line was used at the latter two locations. Eighteen cm^3 of the water samples were filtered with new Minisart 17764-ACK RC 0.2 µm syringe filters and kept in cleaned 20-ml HDPE Zinsser vials. Three internal replicate samples were taken from each deployment.

Near-surface pore in salt marshes and intertidal flats showed a high diurnal and tidal variability (e.g. Baumann et al., 2015), also with reference to desiccation and root respiration of the salt marsh vegetation (e.g. Koop-Jakobsen et al., 2018). We collected pore waters during the ebb period in the morning or in the evening (3-May-2019 only), shortly after the sampling sites emerged, in order to capture an intermediate situation of the daily cycle and not an extreme (Saderne et al., 2013), and to obtain a sufficient sample volume. The pore waters were collected with rhizone samplers at the foraminiferal sampling sites along the salt marsh and tidal flat transect (Dickens et al., 2007). A small rectangular hole of approximately 5 to 7 cm width and depth was dug out. One or two rhizones were inserted oblique upwards in opposite walls of the hole, in that the tip of the rhizone was situated in the uppermost centimetre of the surface sediment, or in the thin oxic layer. A 20-cm^3 syringe was plugged to the luer-lock connector of the rhizone tubing, the syringe piston was pulled to generate a vacuum, and held open with a spacer slat (Seeberg-Elverfeldt et al., 2005). The pore size of the rhizones was 0.1 µm, and 15 to 20 mL pore water was collected in 20 minutes to 3 hours, depending of the water content of the sediment. The in-situ temperature was measured with a plug-in thermometer during pore water extraction.

Sea water and pore water salinities and temperatures were routinely measured with hand-held WTW Cond 3210 or LF320 conductimeters equipped with a TetraCon 325 probe. The precision of the instruments was <0.5% of measured conductivity and <0.1 K according to manufacturer's test certificates (Schönfeld and Mendes, 2021). A calibration of the LF320 conductimeter with sea water standards revealed an accuracy of ±0.116 units (1-sigma).

The pH was measured with a WTW pH 3210 equipped with a WTW Sentix 81 glass electrode, which was calibrated with NIST/DIN buffers pH 1.679, 4.006, 6.865, and 9.180, the precision is ±0.015 units according to manufacturer's data sheets. The buffers were measured before and after each sample series. The differences between measured and expected values ranged from -0.005 to -0,030 units and showed a consistent pattern on each day. Therefore, the sea water and pore water measurements were corrected by an individual, linear regression model for each day. The residual

variance, hence accuracy of the corrected pH measurements was ±0.008 units (1-sigma, n = 40). The variance of internal replicate sea water samples from the same sampling pitcher was <±0.026, on average ±0.010 ph units (±0.1 %), which is very close to the accuracy as obtained from standard measurements. The variance of external replicate pore water samples taken at the same location was <±0.677, on average ±0.137 units (±2.0 %).

The total alkalinity of sea water and pore waters was determined immediately after sampling with the pH method after Andersen and Robinson (1946). The sample volumes as recommended by Grashoff (1976) were reduced by a factor of 5 because of the low yield of pore water extraction. In detail, 15 cm^3 of the water sample was filled in a cleaned 20-mL HDPE Zinsser vial. The conductimeter probe was rinsed with bidistilled water, dried with Kimwipes™, inserted, salinity and temperature of the sample were mesured. The pH electrode was rinsed with bidistilled water, gently dabbed with a Kimwipe™, inserted and the pH of the sample was measured. Thereafter, 10 cm^3 were extracted with a bulb pipet and transferred in a new 20-mL Zinser vial. One cm^3 of 0.025 M HCl was added with a dispenser, the lid of the Zinser vial was fastened, gently shaken, opened and the pH of the acidified sample was measured. The alkalinity was calculated as follows:

$$TA = ((molsol - (POWER(10;(pHac*-1))*aH))*1000000)/d) \quad [\mu mol\ kg^{-1}]$$

molsol is the molarity of the solution measured, i.e. volume HCl * molarity HCL / (sample volume + HCl volume) (0.002272727 in the present case), *pHac* is the pH of the acidified sample, *aH* is the hydrogen activity coefficient in sea water, and *d* is the seawater density in g/cm^3. The hydrogen activity coefficient was interpolated from values provided by Leyendekkers (1973) for the respective temperatures and salinities (Supplement Tab. 1). The seawater density was calculated from measured temperatures and salinities of the samples by using a web-based application (https://www.mt-oceanography.info/Utilities/density.html). The precision of the pH method has been constrained to 0.5 to 1 % (Andersen and Robinson, 1946), or even to 0.1 % (Perez and Fraga, 1987). The variance of 15 internal replicate measurements was <±5.2, on average ±1.6 µmol kg^{-1} (±0.1 %) in our study.

Carbonate system parameters pCO_2 and omega for calcite (Ω Ca) were calculated from pH, TA, temperature, and salinity, by using the CO2SYS software, version 25b06 (Lewis and Wallace, 1998). The phosphate and silicate concentrations were set to 0.8 and 20 µmol kg^{-1} following Brito et al. (2010). The dissociation constants K1 and K2 were chosen according to Lueker et al. (2000) and the $KHSO_4$ dissociation constant after Dickson (1990).

3. Results

3.1 Morphology, sediments and salt marsh flora

The transect investigated commences at a supratidal sand ridge, which is composed of coarse sand with small pebbles and shell debris (Fig. 2). The ridge shows a rather flat crest at 1.9 to 2.1 m POD. It is sparsely vegetated with a heath of low *Salsola vermiculata*. Large bushes of *Limoniastrum monopetalum* and *Suaeda vera* were found at the slopes of the ridge. They stand in groups at distances of ca. 2 to 5 m, which are intersected by non-vegetated sand patches that were shaped in the swash zone of storm surges. The slope base is delineated by the highest occurrences of saltwort halophytes, namely *Arthrocnemum macrostachyum* in exposed, dry areas and *Sacocornia fructicosa* in more sheltered, wet places.

The transect commenced at the highest occurrence of *Arthrocnemum macrostachyum* at 1.64 m POD, which marks the upper limit of the upper salt marsh at 0.02 m below Mens Spring High Water (Figs. 2, 3). The sand patch around transect zero and the footpath were covered by a 2 - 3 cm thick, dark-brown mat of rotten *Zostera noltii* leaf debris (Supplement Tab 2). Coarse sand with shell debris was encountered below. The area was vegetated with single, 60-cm high *Arthrocnemum macrostachyum* in patches and low *Suaeda vera.* The debris mat continued beyond the non-vegetated footpath after 2.8 m and passed into a 3 - 5 cm thick surface layer of humus-rich mud with rotten plant debris, extending until 7.9 or 7.4 m (in 2019), above muddy sand with black and brown spots. The vegetation was dominated by high and dense *Arthrocnemum macrostachyum* (Fig. 3).

Thereafter, the sediment changed into an organic-rich olive-brown mud with an even surface, which was homogenously vegetated with low *Arthrocnemum macrostachyum.* The highest *Halimione portulacoides* was recorded at 18.4 or 18.6 m (in 2019) (Supplement Tab 2), which marked the boundary between the upper and lower salt marsh at an elevation height of 1.20 or 1.22 m POD respectively, 0.1 or 0.08 m below Mean High Water level. First, scattered *Spartina maritima* appeared at 19.0 m. From 21.3 m, the sediment was a

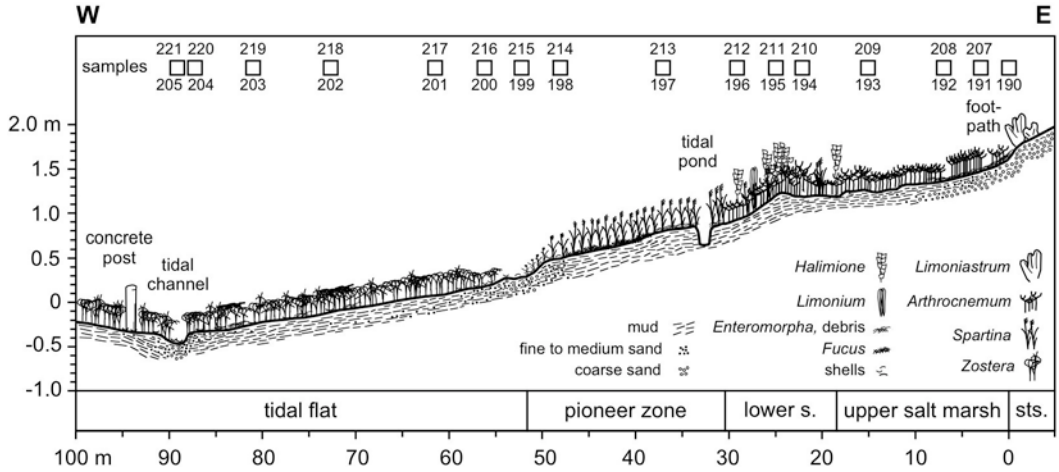

Fig. 3. Sediments, vegetation and sampling sites (squares) along the investigated transect in the north-western Ria Formosa salt marsh in May 2019 (Fig. 2). Numbers below the squares refer to 2018, above to the 2019 sampling campaign. Abbreviations: s: salt marsh, sts: supratidal sand ridge.

soft, grey, organic-rich mud with dark-brown spots, vegetated with high *Arthrocnemum macrostachyum*. *Halimione portulacoides* was common and homogenously distributed beyond 23.7 m. The sediment changed again to grey or brown coloured soft, plastic mud, at 25.8 m and a height of 1.14 m POD, which was vegetated very densely with low, creeping *Arthrocnemum macrostachyum* and scattered *Halimione portulacoides*. A patch of *Limonium vulgare* was encountered 2 - 3 m south of the transect, between 26.8 and 27.7 m (Fig. 3).

A dense vegetation of *Spartina maritima* appeared at 30.3 or 30.6 m (in 2019) marking the boundary of the lower salt marsh and pioneer zone at a height of 0.88 m POD, 0.02 m below Mean Neap High Water. A few runners of *Arthrocnemum macrostachyum* were still found up to 31.3 m (Supplement Tab 2). The sediment was a soft, brown mud, turning black and anoxic a few mm below an uneven surface covered by a patchy mat of *Enteromorpha* sp. and *Fucus vesiculosus*. At 47.5 or 47.2 m (in 2019), the surface sediment changed to a muddy coarse sand with bivalve shells and few pebbles. The redox boundary was recognised a few mm below an hummocky surface. Fiddler crab burrows were common. The vegetation of low *Spartina maritima* was less dense than on the mud before. The lower boundary of the pioneer vegetation zone was recognised at 51.4 or 51.9 m (in 2019) at a height of 0.32 or 0.31 m POD respectively, 0.02 or 0.03 m below Mean Tidal Level (Fig. 3).

A non-vegetated sand flat was recorded from the vegetation boundary up to 58.2 or 56.5 m (in 2019) at a high of 0.15 or 0.17 m POD respectively. The sediment was a greyish-brown coarse sand passing into a muddy sand with an uneven surface and a redox boundary at 5 to 10 mm depth. Gastropod and bivalve shells were found on the surface, fiddler crab burrows and openings of polychaete tubes of 3 - 5 mm diameter were common. The tidal flat continued with a sandy to clayey, soft mud beyond. The redox boundary was recorded a few millimetres below the mostly even surface. The mud flat was vegetated by dense and homogenous *Zostera noltii*, patches of *Enteromorpha* sp., and few *Ulva* sp. in places. A braided tidal channel was present between 88 and 90 m (Figs. 2, 3). It was incised by 14 or 12 cm (in 2019) only. The surface sediment in the channel was a gastropod and bivalve shell-rich muddy sand, patchy vegetated with *Zostera noltii.* Hermit crabs and gastropods were common. The mud flat continued beyond a concrete post overgrown with oysters and barnacles at 94 m, which marks the end of the transect investigated (Fig. 3).

3.2 Hydrography

The high waters recorded during 12 lunar months from 3-June-2019 to 22-May-2020 showed the highest tidal amplitudes during the equinoxes and the lowest amplitudes in December and June (Fig. 4). The Mean High Water level was 1.30 m (n = 683). Mean Spring High Water was 1.66 m, and Mean Neap High Water was 0.90 m POD (n = 96). The pressure sensor of the data logger was situated at 0.61 m POD, and two of 96 neap tides were not recorded. The Mean Tidal Level was constrained to 0.34 m POD in an earlier study (Schönfeld and Mendes, 2021).

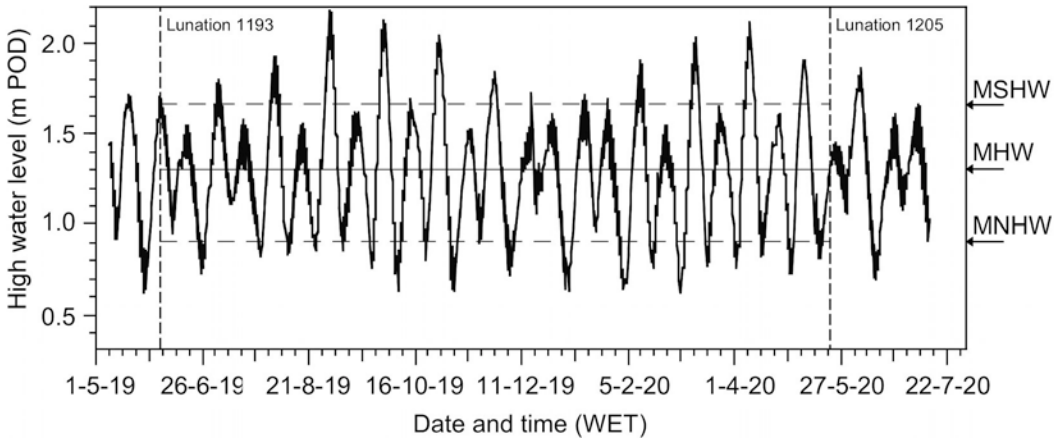

Fig. 4. High water levels in Esteiro do Ancão measured at the hydrographic monitoring station (Fig. 1). Abbreviations: MSHW: Mean Spring High Water, MHW: Mean High Water, MNHW: Mean Neap High Water, WET: Western European Time.

Manually measured salinities and temperatures of Ria Formosa and Gulf of Cadiz waters ranged from 36.0 to 37.6 units and 17.3 to 25.7 °C, with mean values of 36.5 and 20.1 °C in early May 2018 and 2019. Shallow waters at the salt marsh transect were slightly higher in salinity and temperature than Esteiro do Ancão ebb waters, and the latter values were higher than those from the adjacent Gulf of Cadiz (Supplement Table 3).

The 14-months record from the hydrographic monitoring station at Esteiro do Ancão showed a high diurnal variability and long-term fluctuations over several weeks (Supplement Fig. 2). The air temperatures raised to 33.5 °C in summer and fell to 4.5 °C in winter. Esteiro do Ancão high-water temperatures varied between 10.4 and 26.9 °C, and they followed the trend of the air temperatures even though with a lower amplitude. The mean values were 19.4 (n = 833) and 19.5 °C (n = 33937) respectively. The high-water salinities varied between 25.8 and 38.2 units, and were on average 36.5 units (n = 190). Exceptional low values have to be taken with caution as they well may be caused by the growth of biofilms, barnacles, and even by tiny air bubbles on the sensor surface (Richard O'Brian, Dataflow Systems, Christchurch, New Zealand, pers. comm. 5-Sept-2019). None-the-less, the scattered, reliable salinity data with a low difference between the individual sensor readings were in good agreement with manual measurements as given above. The salinity logging data showed systematic variations over several weeks in spring and early summer 2020 (Supplement Fig. 2), which neither correlated with water level nor temperature fluctuations.

3.3 Carbonate chemistry

The pH of surface water samples taken at the salt marsh transect was on average 8.244 and thus slightly higher than in Esteiro do Ancão and Gulf of Cadiz waters, which were 8.094 and 8.049. With reference to higher salinities and pH values, the TA was slightly higher in the Esteiro do Ancão than in the adjacent Gulf of Cadiz, 2209 and 2173 µmol kg^{-1} (Supplement Tab. 4). The mean pCO_2 was 462 µatm in the Esteiro do Ancão and thus higher than the atmospheric partial pressure of 410 µatm at that time though markedly lower than 534 µatm in the near-shore Gulf of Cadiz. It has to be noted, however, that indoor measurements produced slightly higher pCO_2 values than measurements made in the shadow outside. The calcite saturation Ω Ca of Esteiro do Ancão and Gulf of Cadiz waters were 4.6 and 3.7-fold the equilibrium value.

Measurements of near-surface pore waters of tidal flat sediments and salt marsh soils showed a high data variability between the replicates and the 2018 and 2019 campaigns (Fig. 5). The pore water salinities were close to Esteiro do Ancão values near the tidal channel. They successively raised to

41 units in the pioneer zone, and reached a maximum of 49.6 units in the highest salt marsh. The pH values were generally about one unit lower in tidal flat sediments than in the Esteiro do Ancão surface water. They decreased again by 0.3 units at the lower boundary of the pioneer zone and reached a minimum of 5.911 in the lower salt marsh, from where they increased again to 7.427 in the upper salt marsh.

The TA of near-surface pore waters on the tidal flat and in the pioneer zone were slightly higher than the mean TA of Esteiro do Ancão surface waters (Fig. 5). The TA values showed a comparatively low scatter. The data variability increased at the lower salt marsh boundary and spread further in the upper salt marsh. Values from the 2019 sampling were consistently lower than those from 2018. The pCO_2 values were up to 20-fold higher in tidal flat pore waters than in Esteiro do Ancão. They further increased by up to two orders of magnitude at the vegetation boundary. The pore water pCO_2 declined again to the range of tidal flat values in the upper part of the upper salt marsh. The calcite saturation showed a high scatter as well. Ω Ca values of near-surface pore waters were on average 0.78 on the tidal flat, hence moderately undersaturated. The data variability diminished and the values decreased to strongly undersaturated conditions displayed by a mean of 0.24 in the pioneer zone and

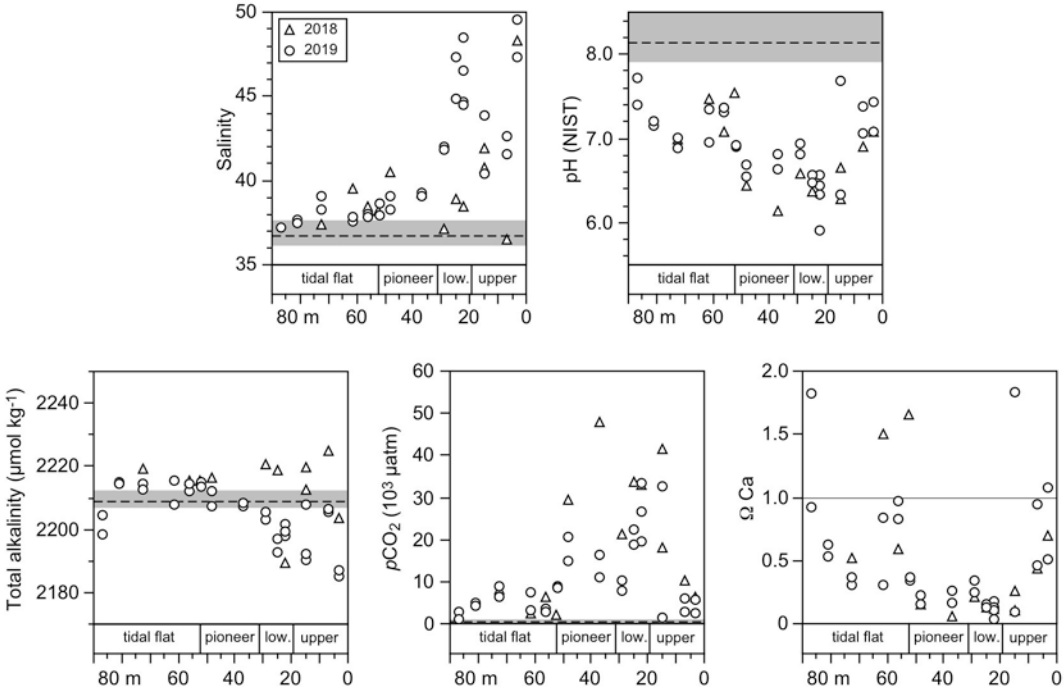

Fig. 5. Salinity, pH and carbonate system parameters of pore waters along the salt marsh transect. Grey box and dashed line: range and mean value of Esteiro do Ancão surface water.

lower salt marsh. In the uppermost salt marsh, pore waters were on average 0.69 and moderately undersaturated again. The uppermost salt marsh data showed a higher variability than in the lower salt marsh and pioneer zone (Fig. 5).

3.4 Organic carbon

The total organic carbon concentrations ranged from 0.4 to 2.3 % on the tidal flat and showed systematically lower values in sand-rich surface sediments. They raised up to 6.2 % in the soft muds of the pioneer vegetation zone and further increased to 11.8 % in the rooted soil of the upper salt marsh. In or underneath the debris mat covering the surface of the highest part of the upper salt marsh, the organic carbon values reached extreme values of 17.1 %, while they were 0.4 % in the sand at the spring high water line. It has to be noted that the Corg values of 2018 samples were consistently lower than those from the 2019 samples (Fig. 6).

3.5 Living benthic foraminifera

In total, 53 different foraminiferal species were recorded in the living fauna (Appendix 1, Plate 1). Twenty-two species were rotaliids, 20 species were textulariids and 11 species were miliolids. Agglutinated species were dominant in the lower and upper salt marsh. They showed rising proportions in the pioneer vegetation zone, and low proportions on the tidal flat (Fig. 6). The faunas

on the tidal flat were dominated by calcareous species, mainly rotaliids. *Ammonia aberdoveyensis, Ammonia tepida, Aubignyna hamblensis, Haynesina depressula, Entzia macrescens, Quinqueloculina bosciana, Quinqueloculina seminulum* and *Trochammina inflata* were the most abundant species (Fig. 6). They comprised on average 77 and 81 % of the living fauna in the salt marsh and pioneer zone, and 58 and 55 % on the tidal flat in 2018 and 2019 respectively. The individual proportions ranged from 0.4 to 82 %, the averages were 22 % in 2018 and 17 % in 2019. Some of them showed proportions of up to 25 % in places. The other species were less abundant (Supplement Tab. 5, 6).

Most of the species were common in marginal marine environments. Only a few were found on continental shelves at mid latitudes, e.g. *Asterigerinata mamilla*, *Bolivina ordinaria, Fissurina lucida*, and *Morulaeplecta bulbosa*. Other species were common in Nordic fjords, e.g. *Ammoscalaria runiana, Eggerella europea, Reophax arctica*, and *Textularia earlandi*. They all were rare on the salt marsh transect investigated.

The highest population densities of 1609 to 8448 individuals per 10 cm^3 were recorded in the upper part of the lower salt marsh and upper salt marsh from 3 to 22 m (Fig. 6). Intermediate and variable values ranging from 123 to 1397 individuals per 10 cm^3 were found in the upper part of the lower salt marsh, pioneer zone and upper part of the tidal flat where sands to sandy muds prevailed until 61.5 m. The lower part of the tidal mud flat and the tidal channel showed low values of 15 to 135 individuals per 10 cm^3. With the exception of samples at 3, 37, and 48 m, the population densities were on average higher by 534 individuals per 10 cm^3 in 2019 than in 2018. The diversities were generally very low. The Fisher alpha indices ranged from 0.9 to 9.3 and showed a successive increase from the salt marsh to the tidal flat (Supplement Tab. 5, 6).

Plate 1. Living (rose-Bengal stained) foraminifera from the tidal flat and salt marsh transect, north-western Ria Formosa, Algarve, Portugal. 1, 2: *Trochammina inflata*, 1 dorsal, 2 ventral view (sample 193). 3, 4: *Entzia macrescens*, 3 dorsal, 4 ventral view (sample 192). 5: *Glomospira gordialis* (sample 211). 6: *Miliammina fusca* (sample 192). 7: *Textularia earlandi* (sample 220). 8: *Affinetrina planciana* (sample 198), not: the aperture is plugges with cytoplasm. 9: *Quinqueloculina seminulum* (sample 215). 10: *Quinqueloculina pseudobuchiana* (sample 220). 11: *Quinqueloculina bosciana* (sample 207). 12: *Fissurina lucida* (sample 199). 13, 14: *Asterigerinata mamilla*, 13 ventral view (sample 200), 14 dorsal view (sample 203). 15: *Bolivina ordinaria* (sample 203). 16, 17: *Ammonia aberdoveyensis*, 16 dorsal view (sample 207), 17 ventral view (sample 198). 18–20: *Buccella granulata*, 18 dorsal view, 19 side view, 20: ventral view (sample 200). 21, 22: *Helenina anderseni*, 21 ventral, 22 dorsal view (sample 214). 23, 24: *Ammonia tepida*, 23 dorsal, 24 ventral view (sample 200). 25, 26: *Aubignyna hamblensis*, 25 dorsal, 26 ventral view (sample 203). 27, 28: *Haynesina germanica*, 27 side view, 28 lateral view (sample 215). 29–31: *Trichohyalus aguayoi*, 29 ventral view, 30 side view, 31 dorsal view (sample 191). 32, 33: *Haynesina depressula*, 32 side view, 33 lateral view (sample 215). 34: *Elphidium cuvillieri*, lateral view (sample 220).

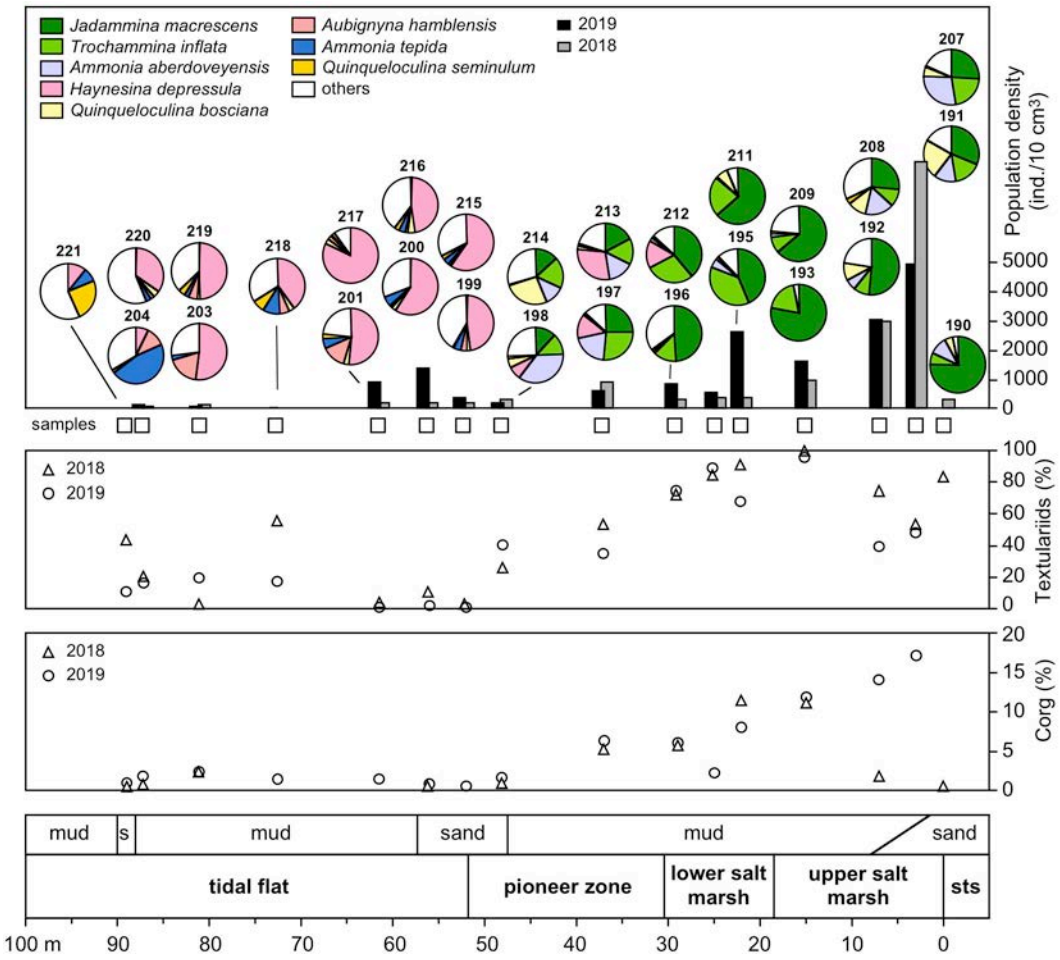

Fig. 6. Vegetation zones, sediments, Corg contents, proportion of textulariids, foraminiferal population densities and abundance of the 2018 and 2019 six-ranked species along the salt marsh transect. The upper pie charts refer to 2019, and the lower pie charts to 2018 samples (Fig. 3). Abbreviations: s: sand, sts: supratidal sand ridge.

Four levels of faunal changes were recognised on the salt marsh transect. The highest samples up to 7 m were characterised by high proportions of *Entzia macrescens*, *Trochammina inflata*, and the calcareous species *Ammonia aberdoveyensis, Trichohyalus aguayoi* and *Quinqueloculina bosciana*. The calcareous species declined in abundance between 7 and 15 m, and *Glomospira gordialis* (*Ammovertellina* sp. of authors) appeared (Supplement Tab. 5, 6). The next level of faunal change was at 22 m, where *Miliammina fusca* declined, *Helenina anderseni* and *Haynesina depressula* appeared, and *Trochammina inflata* increased in abundance. The agglutinated species declined while *Ammonia aberdoveyensis* and *Quinqueloculina bosciana* increased in abundance at 37 m in the pioneer vegetation zone. The most prominent level of faunal change was recognised between 48 and 52 m at the vegetation boundary. *Ammonia aberdoveyensis* changed with *Ammonia tepida. Aubignyna hamblensis* and *Elphidium cuvillieri* appeared, *Haynesina depressula* became consistently very frequent while *Helenina anderseni* disappeared. The agglutinated species *Entzia macrescens* and *Trochammina inflata* disappeared from the transect investigated. The faunas on the tidal flat were rather uniform. In the tidal channel, other species such as *Eggerelloides scaber, Buliminella elegantissima* and different *Quinqueloculina* species were recorded.

3.6 *Ammonia* species dissolution

Ammonia aberdoveyensis was frequent in the upper part, and *Ammonia tepida* was common in the lower part of the salt marsh transect. *Ammonia advena* and *Ammonia batava* were rare and only 1 or 5 individuals of were found in single samples (Supplement Tab. 5, 6). The number of *Ammonia* specimens varied between 2 and 57 living individuals per sample (Supplement Tab 7). Among these,

two, three or even four different preservation stages were recognised. Stages 1 and 2, i.e. intact specimens with a glossy or dull shell, dominated in the upper part of the upper salt marsh (dissolution index 1.4 to 1.7). Stages 3 and four, i.e. damage or loss of one or more chambers, were frequent from the lower part of the upper salt marsh to the pioneer zone (dissolution index 2.0 to 4.0). On the tidal flat, stages 2 and 3 dominated again (dissolution index 1.8 to 2.4) (Supplement Tab. 7).

The index showed a significant negative correlation with Ω Ca of the ambient pore water (n = 23, r = -0.46, p = 0.03) (Fig. 7). It has to be noted that in particular *Ammonia aberdoveyensis* lives in Ria Formosa saltmarsh sediments at calcite saturation levels far below what has been reported from subtidal environments to date (Ω Ca = 0.5), and even below levels which have been created in experimental setups simulating ocean acidification (Ω Ca = 0.33; Haynert et al., 2014).

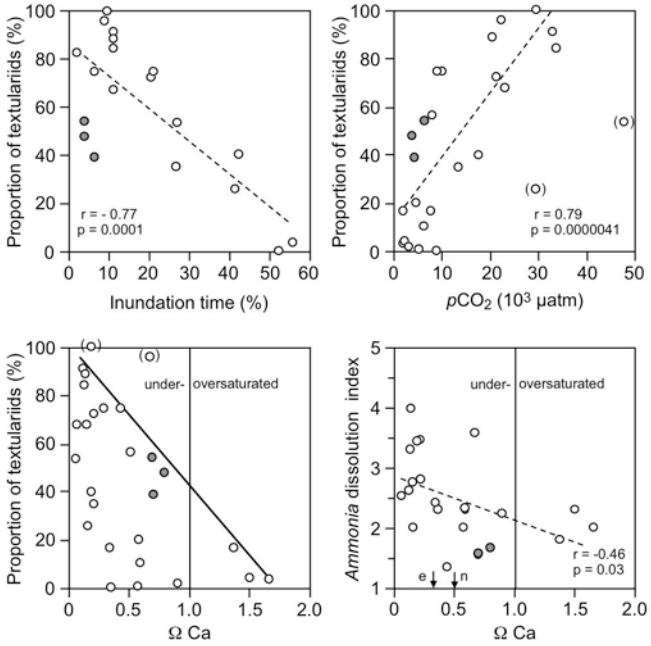

Fig. 7. Comparison of the proportion of textulariids and the *Ammonia* dissolution index with inundation time, pCO_2, and Ω Ca. The dashed line indicates the linear regression, the solid line delineates a data field boundary. Values in brackets are regarded as outliers and were not considered for univariate statistics and interpretation. Grey dots: samples 191, 207, and 208 from a mat of rotten plant debris. Abbreviations: e: lowest experimental level, n: lowest level observed in subtidal environments (Haynert et al., 2014).

4. Discussion

4.1 Salt marsh vegetation zones

The distribution of halophytes in salt marshes are mainly limited by flooding frequency and salinity (Ranwell, 1972; Adam, 1993), which mostly decrease with elevation (Sánchez et al., 1996; Bockelmann et al., 2002). Salt marsh plant zonation schemes were established with reference to the observed species' ranges, (e.g. Heydemann, 1984; de Jong et al., 1998). A belt of highly salt tolerant pioneer vegetation, e.g. *Spartina* or *Salicornia* spp. (e.g. Katschnig et al., 2013), was recognised below MHW. The genuine salt marsh above MHW was usually subdivided into a "low marsh" and "high marsh". The "low marsh" is characterised by a high floral diversity, because most species' niches are centred here (e.g. Suchrow and Jensen, 2010). Indicator species for brackish or dry conditions, e.g. *Juncus*, *Festuca* or *Elymus* spp. delineate the "high marsh" (e.g. Rozema et al., 1978; Bockelmann and Neuhaus, 1999).

This zonation generally applies to the Ria Formosa salt marsh investigated, and the zonal boundaries match characteristic tidal levels. The pioneer zone commenced at 0.32 m POD. This level coincided with MTL at 0.34 m POD, which was inundated during 50 % of the time and twice a day (Supplement Fig. 3). Despite macroalgae*, Spartina maritima* was the only halophyte in the pioneer zone where pore water salinity successively raised from 38 to 40 units (Fig. 5). The base of the lower salt marsh was drawn with the lowest occurrence of *Arthrocnemum macrostachyum* at 0.88 m POD, coinciding with MNHW (Fig. 4). The pore water salinity exceeded 40 units above this level that was submerged

during 23 % of the observation time. The indicator species of the lower salt marsh, *Halimione portulacoides*, showed its landward boundary at 1.22 m POD, 0.08 m below MHW, and at pore water salinities of up to 44 units. This level was flooded during 10 % of the observation time (Supplement Fig. 3). *Arthrocnemum macrostachyum* vanished at 1.64 m POD, close to MSHW at 1.66 m POD, where pore water salinities of >47 units and submergence during 2 % of the observation time was recorded (Fig. 5). Even though the pore water salinity may be subjected to diurnal and seasonal changes, and the inundation frequency is a long-term average, an inverse relationship of these parameters was recognisable. The inverse relationship suggests enhanced evaporation or the extraction of moisture by saltmarsh plants as governing environmental factors. With reference to elevated pore water salinities on the sand flat before the pioneer zone, and higher salinities of Esteiro Ancão ebb waters than in the Gulf of Cadiz, evaporation seems to be of higher importance here. A monospecific high marsh vegetated with *Arthrocnemum macrostachyum* was also found at Tubli Bay, Bahrain, where the evaporation was very high and fresh water sources were absent (Kaminski et al., 2020).

Precipitation and fresh water influence exceeds evaporation in temperate salt marshes, where the interstitial water salinity usually decreases landwards (e.g. Müller Navarra et al., 2016, 2017). Consequently, saltworts of the subfamily Salicornioideae are common in the pioneer zone and low marsh, and grasses of the order Poales are frequent in the high marshes of mid and northern Europe. At Ria Formosa, however, both taxa were missing in the respective vegetation zones and the pore water salinity increased landwards. This offers an explanation for the inverse distribution of Salicornietae, which are among the most salt tolerant plants (Silva et al., 2007; Katschnig et al., 2013). It has to be noted that other factors as nutrient availability, competition, sediment supply, and predation may also influence the distribution of halophyte taxa in salt marshes (e.g. Suchrow, 2014 and references therein). At Venice lagoon, Italy, for instance, no correlation of plant associations with the submergence time and soil salinity was recognised (Silvestri et al., 2005). Instead, a governing influence of root-level oxygen availability modified by evapotranspiration fluxes by the plants and subsurface water flow was suggested. Our observations of oxygenated soil in the Ria Formosa upper salt marsh and subsurface anoxic conditions in the pioneer zone were apparently in agreement with their conclusions.

4.2 Foraminiferal distribution patterns

The foraminiferal species inventory from Ria Formosa salt marsh transect largely resembles the living fauna from Ancão Peninsula backbarrier beach transect (Schönfeld and Mendes, 2021). However, 10 of 53 species recorded at the salt marsh have not been found at the backbarrier beach. Only two of them, *Arenoparrella mexicana* and *Haplophragmoides manilaensis* were considered as genuine salt marsh species (e.g. Lehmann, 2000). Five of the eight other species that were not recorded at Ancão Peninsula have been reported from the eastern Mediterranean, mainly at high salinities, e.g. *Affinetrina planciana*, *Buccella granulata* and *Quinqueloculina pseudobuchiana* (e.g. Cimerman and Langer, 1991; Mateu-Vicens et al., 2010; Mouanga, 2017), or at extreme and variable environmental conditions, e.g. *Bisaccium imbricatum* and *Helenina anderseni* (e.g. Flako-Zaritzky et al., 2011; van Hengstum and Scott, 2011). This also applies to *Trichohyalus aguayoi* (e.g. Berkley et al., 2008; Kaminski et al., 2020). In general, the succession of species along the Ria Formosa salt marsh transect largely resembles distributions recorded at Mediterranean microtidal environments (Debenay and Guillou, 2002, there Fig. 1F), where evaporation exceeds precipitation (e.g. Mariotti, 2010; Romanou et al., 2010), and in Bahrain (Kaminski et al., 2020). A negative hydrologic balance is also recognised for southern Iberian including the Algarve region (e.g. Stigter et al., 1998; Páscoa et al., 2017).

The levels of foraminiferal faunal changes at the Ria Formosa salt marsh transect coincide only in part with the vegetation zonal boundaries or characteristic tidal levels. This concerns the level at 22 m in section and 1.20 m POD, where *Trochammina inflata* increased in abundance, and *Helenina anderseni* and *Haynesina depressula* appeared (Supplement Tab. 5, 6). The top of the lower salt marsh as indicated by the highest occurrence of *Halimione portulacoides* was recognised at 1.22 m POD and 0.08 m below MHW. The most prominent level of faunal change was recorded between 0.50 and 0.31 m POD at the base of the pioneer vegetation zone and MTL, where the salt marsh species *Entzia macrescens* and *Trochammina inflata* disappeared, and the tidal flat fauna with *Haynesina depressula, Ammonia tepida, Aubignyna hamblensis,* and *Elphidium cuvillieri* established

(Supplement Tab. 5, 6). A similar faunal change with an increase in abundance of *Haynesina depressula* was recognised at 15 m in section and 0.20 m POD at the Ancão Peninsula backbarrier transect (Schönfeld and Mendes, 2021), albeit 0.14 m below MTL. Such variations in the elevation of foraminiferal zonal boundaries at short distances were found to increase with tidal amplitude (Francescangeli et al., 2017), and they are not due to levelling inaccuracies.

The other levels of faunal changes at the Ria Formosa salt marsh transect were rather related to sedimentary and pore water properties than to tidal characteristics or vegetation zones. The highest level at 7 m in section and 1.36 m POD, where the calcareous species *Ammonia aberdoveyensis, Trichohyalus aguayoi* and *Quinqueloculina bosciana* declined, is characterised by a decrease of Ω Ca values from more than 0.68 to less than 0.19, even though this change in pore water chemistry was recognised at 15 m in 2019 (Supplement Tab. 7). The high Ω Ca values above were seemingly related to a mat of rotten plant debris covering the surface (Supplement Tab. 2). The level of faunal change at 37 m and 0.81 m POD, where the agglutinated species declined, and *Ammonia aberdoveyensis* and *Quinqueloculina bosciana* increased in abundance, coincided with a marked decrease in Corg contents of more than 5.0 % above and less than 1.6 % below (Supplement Tab. 7). The faunal change at 37 m was also accompanied by a decrease in foraminiferal population densities (Fig. 6), even though a robust covariance of population densities and Corg was not recognised. It is generally accepted that a high availability of labile organic material, e.g. phytoplankton, stimulates growth and reproduction of benthic foraminifera and thus may lead to higher population densities (e.g. Gustafsson and Nordberg, 1999; Nomaki et al., 2005; Schönfeld and Numberger, 2007). Salt marsh sediments contain, however, a high and variable proportion of refractory organic matter, which is of low nutritional value for benthic foraminifera (e.g. Armynot du Châtelet et al., 2009; Leorri et al., 2018). Therefore, the relationship of salt marsh foraminiferal abundances and Corg has to be interpreted with caution (Bouchet et al., 2021).

4.4 Foraminiferal response to pore water chemistry

The agglutinated species *Trochammina inflata* and *Entzia macrescens* were the dominant faunal constituents in the vegetated zone of the Ria Formosa salt marsh transect. They showed exceptionally high population densities and proportions increasing from the pioneer zone to the upper salt marsh (Fig. 6), a very similar pattern as observed in the Ria Guadiana estuary (Camacho et al., 2015a). Both species may withstand long times of subarial exposure and permanently carbonate-undersaturated conditions (Murray and Alve, 2011; Francescangeli et al., 2017). Indeed, and grouped with other textulariids, they showed a significant negative correlation with inundation time, which was weakened by those very three samples from the debris mat on the sediment surface in the highest salt marsh (Fig. 7). The proportion of textulariids showed a correlation of higher significance with pore water pCO_2, however, with the debris mat samples included (Fig. 7). This pattern demonstrates that rather pore water chemistry than elevation in the tidal frame or inundation frequency exerts a governing influence on the agglutinated foraminiferal assemblages at the Ria Formosa salt marsh.

The high scatter of pore water pH, TA, and Ω Ca in the vegetated zones (Fig. 5), and pCO_2 levels two orders of magnitude higher than Esteiro do Ancão waters or the atmosphere raised the question of data reliability. A seasonal variability may be excluded because the 2018 and 2019 sample series were both taken in early May. A diurnal variability is also less likely because both sample series were taken in the morning or in the evening after successive emergence during the ebb period. Our observations and literature evidences rather suggest a spatial heterogeneity created by burrows or roots, which sustains the coexistence of cm-scale patches in the soil with a different redox state (e.g. Koretsky et al., 2005; Koop-Jakobsen et al., 2018), particularly displayed by black or brown mottles (Supplement Tab. 2). The foraminiferal sampling tube had an inner diameter of 35 mm. The rhizone sampled pore water from a spherical space of ca. 16 mm diameter around the tip (Seeberg-Elverfeldt et al., 2005). Consequently, a volume of distinct pore water or faunal properties is sampled, and no integration over an area including all redox states or faunal inhomogenities may be achieved (e.g. Lehmann, 2000; de Chanvalon et al., 2015). With reference to pCO_2, salt marsh soils generally export CO_2 from microbial oxic respiration (Wang et al., 2016). Emerged soils emit one order of magnitude more CO_2 than in a submerged state. Inundation had a higher effect on CO_2 emissions than changes in salinity of the receiving waters (Wang et al., 2019). The calculated pCO_2 values from our study are therefore considered to be in a realistic scale. The Ω Ca values are difficult to compare, because earlier measurements refer to the calcite saturation index (SI) (e.g. Moreno et al., 2007).

The proportion of textulariids showed an inverse relationship with Ω Ca and a confined data distribution (Fig. 7). The distribution displays a minimum proportion of calcareous foraminifers at a given saturation state. This pattern is corroborated by the commonly made observation that calcareous foraminifers may well live in the salt marsh but are scarcely preserved in the dead or fossil assemblages (e.g. Horton and Murray, 2007; Hayward et al., 2014; Camacho et al., 2015b). If there is always a number of calcareous foraminifera present that cope well with high pCO_2 and low calcite saturation in lower and upper salt marsh pore waters, the species concerned must have certain, yet unknown physiological abilities or ecological strategies (Khanna et al., 2013). This applies in particular for *Helenina anderseni* and *Trichohyalus aguayoi*, which have been identified as euryhaline species in earlier studies as discussed above. In contrast to Rio Guadiana estuary (Camacho et al., 2015a), *Ammonia aberdoveyensis* is common in the Ria Formosa salt marsh as well, even though the tests show strong corrosion in places. Indeed, the *Ammonia* dissolution index showed a significant negative correlation with Ω Ca (Fig. 7). This relationship validates and extends the results of earlier laboratory studies on *Ammonia* test dissolution (Le Cadre et al., 2003; Haynert et al., 2011). The occurrence of *Ammonia aberdoveyensis* in the salt marsh is not likely an effect of displacement of living individuals by tidal currents or storm surges (e.g. Murray et al., 1982; Hayward et al., 2004), because this species was very rare in lower intertidal environments (Schönfeld and Mendes, 2021). Therefore, it is justified to assume that the micro-spatial inhomogeneity of pore water chemical properties provides niches for *Ammonia aberdoveyensis,* and other calcareous species, to survive in areas with extreme carbonate undersaturation.

5. Conclusions

The subdivision of a pioneer vegetation zone, lower, and upper salt marsh could be applied at Ria Formosa, as in other European salt marshes. The vegetation zonal boundaries match average high water levels. Mediterranean halophytic taxa and the dominance of saltworts from the subfamily Salicornioideae at Ria Formosa indicate evaporation as governing environmental factor in a lagoon with no significant riverine freshwater influx and a negative hydrologic balance under warm climatic conditions of the Algarve region. This conclusion is corroborated by high and landward increasing pore water salinities in the salt marsh soil.

The carbonate system parameters from Gulf of Cadiz and Esteiro do Ancão surface waters, and pore waters of the tidal flat and salt marsh transect identified the anoxic sediments of tidal flats as source of TA that was exported from the lagoon during each tidal cycle. The salt marsh pore waters were characterised by a high data variability of carbonate system parameters. The scatter was most likely due to small-scale spatial heterogeneities induced by burrows and roots. In general, TA was lower in the salt marsh than on the mud flat, and pCO_2 values were extremely high. The latter were probably fuelled by microbial respiration under subarial exposure during 77 % of the time during one lunar year. Consequently, calcite saturation in the salt marsh soil was far below levels created in experimental setups simulating ocean acidification. A debris mat covering the sediment surface of the highest salt marsh provided sufficient moisture to depress CO_2 production underneath, and to rise the calcite saturation state at the surface to levels comparable to those prevailing on the tidal flat.

The benthic foraminiferal faunas on the tidal flat were dominated by near-shore, calcareous species. Agglutinated salt marsh species were confined to the vegetated zones. Their proportion and population density increased with elevation, while calcareous species again increased in abundance in the highest samples from the upper salt marsh. The majority of the 53 foraminiferal species recorded at the transect has already been reported from Ria Formosa, while 10 species have not been found to date. Most of them were either specialised to high salinities, as prevailing in the eastern Mediterranean, or to extreme and variable environmental conditions. The succession of species along the transect investigated resembled distributions recorded at Mediterranean microtidal environments. None-the-less, only two of four faunal change levels at the Ria Formosa salt marsh coincide with vegetation zonal boundaries, MTL or MHW levels. The other faunal changes were related to changes in Ω Ca and Corg contents. The proportion of textulariids showed a significant negative correlation with submergence time, hence elevation in the tidal frame, and a highly significant correlation with pore water pCO_2. The Ω Ca data and *Ammonia* dissolution indices suggested that a certain number of specimens from highly specialised calcareous species was always present, even at lowest calcite saturation levels.

Our initial hypothesis was verified: pore water carbonate system parameters were exerting a governing influence on the distribution of foraminiferal species in the salt marsh. Salinity or inundation frequency in the tidal frame were of minor importance. It is a matter of further investigation whether small-scale spatial variations of pore water properties provide niches for calcareous species to sustain under generally carbonate undersaturated conditions, or whether they are enabled to live there by physiological adaptations.

Acknowledgements

Óscar Ferreira and Margarida Ramires, Universidade do Algarve, Faro, provided high reference data, D-GPS measurements, support and advice. Anke Dettner-Schönfeld did the levelling in the field. Anke Bleyer and Bettina Domeyer, GEOMAR, Kiel, measured the Corg contents of samples from Ria Formosa salt marsh transect, and provided utensils for pore water sampling. Boie Bogner and Kristin Haynert, GEOMAR, Kiel, introduced the senior author to alkalinity measurements and carbonate system chemistry. Sebastian Beil gave access to the photomicroscope at the Micropaleontological Unit of the Institute of Geosciences, Kiel University. Their help and encouragements are gratefully acknowledged. Isabel Mendes thanks to Fundação para a Ciência e a Tecnologia for Research Assistant contract DL57/2016/CP1361/CT0009 and project UID/0350/ 2020 CIMA.

Appendix 1. Benthic foraminiferal reference list

Note: the type references can be found in WORMS (2022) or Ellis and Messina (1940) catalogues. They are not included in the reference list of the present paper.

Affinetrina planciana (d'Orbigny) = *Triloculina planciana* d'Orbigny, 1839, p. 173, pl. 9, figs. 17, 18.

Ammonia aberdoveyensis Haynes 1973, p. 184, fig. 38, nos. 1-7, pl. 18, fig. 15. Note: Camacho et al. (2015a) discerned two morphotypes at Rio Guadiana (*Ammonia* sp2 and sp3), which both were assigned to genotype T2, i.e. *A. aberdoveyensis* following Hayward et al. (2021). Mainly morphotype sp3 and scarcely sp2 was recorded in the present study. As both were affiliated with the same genotype, they were not discriminated herein.

Ammonia advena (Cushman) = *Discorbis advena* Cushman, 1922, p. 40. Note: *Ammonia limnetes* (Todd and Brönnimann 1957) is considered a junior synonym of *A. advena* by Hayward et al. (2021).

Ammonia batava (Hofker) = *Streblus batavus* Hofker ,1951, p. 498–502, figs. 335, 340, 341

Ammonia tepida (Cushman) = *Rotalia beccarii* var*. tepida* Cushman, 1926, p. 79, pl. 1. Note: the distribution of the respective genotype T20 has been reported as confined to the Caribbean and subtropical western Atlantic (Hayward et al., 2021). There is recent evidence for an occurrence of *A. tepida* in the Mediterranean (Schönfeld et al., 2021).

Ammoscalaria runiana (Heron-Allen and Earland) = *Haplophragmium runianum* Heron-Allen and Earland, 1916, p. 224, pl. 40, figs. 15-18. Note: the retilinear stage is scarcely developed in species found at Ria Formosa salt marsh transect.

Ammotium salsum (Cushman and Bronnimann) = *Ammobaculites salsus* Cushman and Bronnimann, 1948, p. 16, pl. 3, figs. 7-9.

Arenoparrella mexicana (Kornfeld) = *Trochammina inflata* (Montagu) var. *mexicana* Kornfeld, 1931, p. 86, pl. 13, fig. 5.

Asterigerinata mamilla (Williamson) = *Rotalina mamilla* Williamson, 1858, p. 54, pl. 4, figs. 109-111.

Aubignyna hamblensis Murray, Whittaker and Alve 2000, p. 64, pl. 2, figs. 1-16, Fig. 1, a-c, e. Note: *Discorbis* sp. of Camacho et al. (2015a).

Bisaccium imbricatum Andersen 1951, p. 581, pl. 33, figs. 2a, b. Note: this rare species has been recorded from a brackish pond in Israel by Flako-Zaritsky et al. (2011).

Bolivina italica Cushman 1936, p. 56, pl. 8, fig. 6.

Bolivina ordinaria Phleger and Parker 1952, (new name for *Bolivina simplex* Phleger and Parker, 1951, p. 14, pl. 7, fig. 4-6).

Bolivina striatula Cushman 1922, p. 27, pl. 3, fig. 10.

Buccella granulata (di Napoli) = *Eponides frigidus* (Cushman) var. *granulatus* di Napoli, 1952, p. 103, pl. 5, figs. 3, 3a, b.

Buliminella elegantissima (d'Orbigny) = *Bulimina elegantissima* d'Orbigny, 1839, p. 51, pl. 7, figs. 13-14.

Cornuspira involvens (Reuss) = *Operculina involvens* Reuss, 1850, p. 370, pl. 46, fig. 20.

Crithionina granum Goës 1894, p. 15, pl. 3, figs. 28-33.

Crithionina mamilla Goës, 1894, p. 15, pl. 3, figs. 34-36.

Eggerella europea (Christiansen) = *Verneuilina europeum* Christiansen, 1958, p. 66. (new name for *Verneuilina advena* Cushman emend. Höglund, 1947, pl. 13, figs. 11a-c, text fig. 169.)

Eggerelloides scaber (Williamson) = *Bulimina scabra* Williamson 1858: p. 65, pl. 5, figs. 136-137.

Elphidium advenum (Cushman) = *Polystomella advena* Cushman 1922, p. 56, pl. 9, figs. 11-12. Note: the keel is less developed in specimens from Ria Formosa salt marsh transect.

Elphidium cuvillieri Levy 1966, p. 5, pl. 1, fig. 6, pl. 2. Note: *Elphidium poeyanum* of Camacho et al. (2015a).

Elphidium oceanensis (d'Orbigny) = *Polystomella oceanensis* d'Orbigny 1826, p. 285, no. 8. Note: the illustration was provided by Fornasini (1904), p. 13, pl. 3, fig. 10. *Elphidium gunteri* of authors.

Elphidium williamsoni Haynes 1973, p. 207, pl. 24, fig. 7, pl. 25, figs. 6, 9, pl. 27, figs. 1-3.

Fissurina lucida (Williamson) = *Entosolenia marginata* var. *lucida* Williamson, 1848, p. 17, pl. 2, fig 17.

Glomospira gordialis (Jones and Parker) = *Trochammina squamata* (Jones and Parker) var. *gordialis* Jones and Parker, 1860, p. 304. Note: *Ammovertellina* sp. of Camacho et al. (2015a). The irregular, meandering shape of the last chamber part is always attached to the earlier part of the test and thus rather resembles *Glomospira charoides* than the genus type species *Ammovertellina prima.*

Haplophragmoides manilaensis Andersen 1953, p. 22, pl. 4, fig. 8.

Haynesina depressula (Walker and Jacob 1798) = *Nautilus depressulus* Walker and Jacob, p. 641, pl. 14, fig. 33.

Haynesina germanica (Ehrenberg) = *Nonionina germanica* Ehrenberg 1840: p. 23, pl. 2, figs. 1a–g.

Helenina anderseni (Warren) = *Pseudoeponides anderseni* Warren, 1957, p. 39, pl. 4, figs. 12-15.

Entzia macrescens (Brady) = *Trochammina inflata* (Montagu) var. *macrescens* Brady 1870: p. 290, pl. 11, figs. 5a–c. Note: the species has been affiliated with the genus *Jadammina* by authors. Based on morphological characteristics, Filipescu and Kaminski (2011) demonstrated that *Jadammina* is a junior synonym of *Entzia*. Indeed, genetic sequences of living *Entzia macrescens* from Turda, Romania, i.e. the type locality of *Entzia tetrostomella* von Daday (1883), and from Dovey Estuary, United Kingdom, were identical (Holzmann and Pawlowski, 2017). The latter is not the type locality of *Jadammina polystoma* Bartenstein and Brand (1938) but Jade Bight, Germany. To our knowledge, topotypic specimens of *Jadammina polystoma* were not sequenced to date. The proof of identicalness of topotypic gene sequences from both genera is therefore still pending. This appears to be necessary, because morphologically identical specimens of *Entzia macrescens* from Carmargue, southern France, belonged to a new, cryptic species (Holzmann and Pawlowski, 2017).

Lepidodeuterammina ochracea (Williamson) = *Rotalina ochracea* Williamson, 1858, p. 55, pl. 4, fig. 112, pl. 5, fig. 113.

Leptohalysis scotti (Chaster 1892) = *Reophax scottii* Chaster, p. 57, pl. 1, fig. 1.

Miliammina fusca (Brady) = *Quinqueloculina fusca* Brady 1870: p. 286, pl. 11, fig. 2a-c.

Miliolinella hybrida (Terquem) = *Quinqueloculina hybrida* Terquem 1878, p. 79, pl. 9, figs. 23a-c.

Morulaeplecta bulbosa Höglund 1947, p. 165, figs. 142a, b, pl. 12, figs. 2a, b.

Neoconorbina terquemi (Rzehak) = *Discorbina terquemi* Rzehak, 1888, p. 228. Note: new name for *Rosalina orbicularis* Terquem 1876.

Quinqueloculina bosciana d'Orbigny 1839, p. 191, pl. 11, figs. 22–24. Note: Miliolid sp. 2 and 3 of Camacho et al. (2015a).

Quinqueloculina laevigata d'Orbigny 1826, p. 143, pl. 3, figs. 31–33.

Quinqueloculina lata Terquem 1876, p. 82, pl. 11, fig. 8.

Quinqueloculina limbata Fornasini 1905, p. 66, pl. 3, fig. 9. Note: Miliolid sp. 8 of Camacho et al. (2015a).

Quinqueloculina parvula Schlumberger 1894, p. 255, pl. 3, figs. 8-9, text fig. 1.

Quinqueloculina pseudobuchiana Luczkowska 1974, p. 58, pl. 4, fig. 5, pl. 5, figs. 1, 2. Note: Miliolid sp. 6 of Camacho et al. (2015a).

Quinqueloculina seminulum (Linné 1758) = *Serpula seminulum* Linné, p. 786.

Reophax arctica Brady 1881, p. 405, pl. 21, fig. 2. Note: *Cuneata arctica* (Brady 1881) of authors.

Reophax moniliformis Siddall 1886, p. 54, pl. 1, fig. 2.
Reophax nana Rhumbler 1911, p. 182, pl- 8, figs. 6-12. Note: this species differs from *R. arctica* by its brown chamber wall troughout, more distinct, globular chambers, and smaller grains used for the agglutination.
Siphotrochammina lobata Saunders 1957, p. 9, pl. 3, figs. 1, 2. Note: *Siphotrochammina* sp. of Camacho et al. (2015a, b).
Textularia earlandi Parker 1952, p. 458, pl. 2, figs. 4-5. Note: The species has been determined as *Textularia tenuissima* Earland 1933 by authors.
Trichohyalus aguayoi (Bermúdez) = *Discorbis aguayoi* Bermúdez, 1935, p. 204, pl. 15, figs 10-14. Note: *Discorinopsis aguayoi* of authors.
Triloculina oblonga (Montagu) = *Vermiculum oblongum* Montagu 1803, p. 522, pl. 14, fig. 9.
Trochammina inflata (Montagu) = *Nautilus inflatus* Montagu, 1808, p. 81, pl. 18, fig. 3.

References

Adam, P., 1993. Salt Marsh Ecology. Cambridge University Press, Melbourne, 476 pp.
Alison, N., Austin, W., Paterson, D., Austin, H., 2010. Culture studies of the benthic foraminifera *Elphidium williamsoni*: evaluating pH, and inter-individual effects on test Mg/Ca. Chemical Geology 274, 87–93.
Alves da Silva, A.A., Freire, E., Gonçalo Crisóstomo, G., 2008. Variações do nível médio anual do mar em Cascais: características e tendências. Estudos do Quaternário 5, 51–66.
Amergian, K.E., Beckwith, S., Gfatter, C., Selden, C., Hallock, P., 2020. Can areas of high alkalinity freshwater discharge provide potential refugia for marine calcifying organisms? Journal of Foraminiferal Research 52, 60–73.
Anderson, D.H., Robinson, R.J., 1946. Rapid electrometric determination of the alkalinity of sea water. Industrial and Engineering Chemistry 18, 767–769.
Andrade, C., Freitas, M.C., Moreno, J., Craveiro, S.C., 2004. Stratigraphical evidence of late Holocene barrier breaching and extreme storms in lagoonal sediments of Ria Formosa, Algarve, Portugal. Marine Geology 210, 339–362.
Aníbal, J., 2019. Ecological dynamics of green macroalgae Ulvales in Ria Formosa: a tale of blooms and shapes. In: Aníbal, J., Gomes, A., Mendes, I., Moura, D. (Eds.), Ria Formosa: Challenges of a Coastal Lagoon in a Changing Environment, first ed. University of Algarve, Faro, pp. 83–98.
Armynot du Châtelet, E., Bout-Roumazeilles, V., Riboulleau, A., Trentesaux, A., 2009. Sediment (grain size and clay mineralogy) and organic matter quality control on living benthic foraminifera. Revue Micropaleontologie 52, 75–84.
Asmus, R.M., Martin Sprung, M., Asmus, H., 2000. Nutrient fluxes in intertidal communities of a South European lagoon (Ria Formosa) – similarities and differences with a northern Wadden Sea bay (Sylt-Rømø Bay). Hydrobiologia 436, 217–235.
Barbosa, A.B., 2010. Seasonal and interannual variability of planktonic microbes in a mesotidal coastal lagoon (Ria Formosa, SE Portugal): impact of climatic changes and local human influences. In: Paerl, H., Kennish, M. (Eds.), Coastal Lagoons: Critical Habitats of Environmental Change. CRC Press, Taylor & Francis Group, Marine Science Book Series, Boca Raton, pp. 335–366.
Barnett, R.L., Garneau, M., Bernatchez, P., 2016. Salt-marsh sea-level indicators and transfer function development for the Magdalen Islands, Gulf of St. Lawrence, Canada. Marine Micropaleontology 122, 13–26.
Baumann, H., Wallace, R.B., Tagliaferri, T., Gobler, C.J., 2015. Large natural pH, CO_2 and O_2 fluctuations in a temperate tidal salt marsh on diel, seasonal, and interannual time scales. Estuaries and Coasts 38, 220–231.
Berkeley, A., Perry, S C.T., Smithers, G., Horton, B.P., 2008. The spatial and vertical distribution of living (stained) benthic foraminifera from a tropical, intertidal environment, north Queensland, Australia. Marine Micropaleontology 69, 240–261.
Bockelmann, A.-C., Neuhaus, R., 1999. Competitive exclusion of *Elymus athericus* from a high stress habitat in a European salt marsh. Journal of Ecology 87, 503–513.
Bockelmann, A.C., Bakker, J.P., Neuhaus, R., Lage, J., 2002. The relation between vegetation zonation, elevation and inundation frequency in a Wadden Sea salt marsh. Aquatic Botany 73, 211–221.

Bouchet, V.M.P., Frontalini, F., Francescangeli, F., Sauriau, P.-G., Geslin, E., Martins, M.V.A., Almogi-Labin, A., Avnaim-Katav, S., Di Bella, L., Cearreta, A., Coccioni, R., Costelloe, A., Dimiza, M.D., Ferraro, L., Haynert, K., Martínez-Colón, M., Melis, R., Schweizer, M., Triantaphyllou, M.V., Tsujimoto, A., Wilson, B., Armynot du Châtelet, E., 2021. Indicative value of benthic foraminifera for biomonitoring: Assignment to ecological groups of sensitivity to total organic carbon of species from European intertidal areas and transitional waters. Marine Pollution Bulletin 164, 112071, 18 pp.

Bradshaw, J.S., 1961. Laboratory experiments on the ecology of Foraminifera. Contributions Cushman Foundation of Foraminiferal Research 12, 87–106.

Bradshaw, J.S., 1968. Environmental parameters and marsh foraminifera. Limnology and Oceanography13, 26–38.

Brito, A., Newton, A., Tetta, P., Fernandesa, T.F., 2010. Sediment and water nutrients and microalgae in a coastal shallow lagoon, Ria Formosa (Portugal): Implications for the Water Framework Directive. Journal of Environmental Monitoring 12, 318–328.

Cabeçadas, L., Oliveira, A.P., 2005. Impact of a *Coccolithus braarudii* bloom on the carbonate system of Portuguese coastal waters. Journal of Nannoplankton Research 27, 141–147.

Cai, W.J., Hu, X., Huang, W.J., Jiang, L.Q., Wang, Y., Peng, T.H., Zhang, X., 2010. Alkalinity distribution in the western North Atlantic Ocean margins. Journal of Geophysical Research 115, C08014, 15 pp.

Camacho, S., Delminda, M., Connor, S., Scott, D.B., Boski, T., 2015a. Taxonomy, ecology and biogeographical trends of dominant benthic foraminifera species from an Atlantic-Mediterranean estuary (the Guadiana, southeast Portugal). Palaeontologia Electronica, 18.1.17A, 27pp.

Camacho, S., Delminda, M., Simon, C., Scott, D., Boski, T., 2015b. Ecological zonation of benthic foraminifera in the lower Guadiana Estuary (southeastern Portugal). Marine Micropaleontology 112, 1–18.

Carrasco, A.R., Matias, A., 2019. Backbarrier shores along the Ria Formosa lagoon. In: Aníbal, J., Gomes, A., Mendes, I., Moura, D. (Eds.), Ria Formosa: Challenges of a Coastal Lagoon in a Changing Environment, first ed. University of Algarve, Faro, pp. 17–28.

Carrasco, A.R., Kombiadou, K., Amado, M., Matias, A., 2021. Past and future marsh adaptation: Lessons learned from the Ria Formosa lagoon. Science of the Total Environment 790, 148082, 15 pp.

Cearreta, A., Irabien, M.J., Ulibarri, I., Yusta, I., Croudace, I.W., Cundy, A.B., 2002. Recent salt marsh development and natural regeneration of reclaimed areas in the Plentzia estuary, N. Spain. Estuarine, Coastal and Shelf Science 54, 863–886.

Cearreta, A., Murray, J.W., 2000. AMS 14C dating of Holocene estuarine deposits: consequences of high energy and reworked foraminifera. The Holocene 10, 155–159.

Cimerman, F., Langer, M.R., 1991. Mediterranean foraminifera. Slovenska Akademija Znanosti in Umetnosti. Academia Scientiarum et Artium Slovencia, Classis 4, Historia Naturalis, 30, 1–118.

Costa, J.C., Arsénio, P., Monteiro-Henriques, T., Neto, C., Pereira, E., Almeida, T., Izco, J., 2009. Finding the boundary between Eurosiberian and Mediterranean salt marshes. Journal of Coastal Research SI56, 1340–1344.

Costa, J.C., Lousá, M., Espírito Santo, M.D., 1996. Vegetação do Parque Natural da Ria Formosa. Studia Botanica 15, 69–157.

Cravo, A., Jacob, J., 2019. Role of the Ria Formosa inlets on the physical, chemical and biological exchanges with the adjoining ocean. In: Aníbal, J., Gomes, A., Mendes, I., Moura, D. (Eds.), Ria Formosa: Challenges of a Coastal Lagoon in a Changing Environment, first ed. University of Algarve, Faro, pp. 29–46.

de Chanvalon, T.A., Metzger, E., Mouret, A., Cesbron, F., Knoery, J., Rozuel, E., Launeau, P., Nardelli, M.P., Jorissen, F.J., Geslin, E., 2015. Two-dimensional distribution of living benthic foraminifera in anoxic sediment layers of an estuarine mudflat (Loire estuary, France). Biogeosciences 12, 6219–6234.

de Jong, D.J., K.S. Dijkema, J.H. Bossinade, and J.A.M. Janssen. 1998. SALT97. In Classificatieprogramma voor Kweldervegetaties. Rijkswaterstaat RIKZ, Dir. Noord-Nederland, Meetkundige Dienst; IBN-DLO, Nederland.

de la Paz, M., Gómez-Parra, A., Forja, J., 2007. Inorganic carbon dynamic and air-water CO2 exchange in the Guadalquivir Estuary (SW Iberian Peninsula). Journal of Marine Systems 68, 265–277.

de la Paz, M., Gómez-Parra, A., Forja, J., 2008. Tidal-to-seasonal variability in the parameters of the carbonate system in a shallow tidal creek influenced by anthropogenic inputs, Rio San Pedro (SW Iberian Peninsula). Continental Shelf Research 28, 1394–1404.

de los Santos, C.B., Lahuna, F., Silva, A., Freitas, C., Martins, M., Carrasco, A.R., Santos, R., 2022. Vertical intertidal variation of organic matter stocks and patterns of sediment deposition in a mesotidal coastal wetland. Estuarine Coastal and Shelf Science 272, 107896, 9pp.

De Rijk, S., 1995. Salinity control on the distribution of salt-marsh foraminifera (Great Marshes, Massachusetts). Journal of Foraminiferal Research 25, 156–166.

De Rijk, S., Troelstra, S.R., 1997. Salt marsh foraminifera from the Great Marshes, Massa- chusetts: environmental controls. Palaeogeography Palaeoclimatology Palaeoecology 130, 81–112.

Debenay, J.-P., Guillou, J.J., 2002. Ecological transitions indicated by foraminiferal assemblages in paralic environments. Estuaries 25, 1107–1120.

Dickens, G.R., Koelling, M., Smith, D.C., Schnieders, L. and the IODP Expedition 302 Scientists Party, 2007. Rhizon sampling of pore waters on Scientific Drilling Expeditions: an example from the IODP Expedition 302 (ACEX). Scientific Drilling 4, 22–25.

Dickson, A. G. 1990. Standard potential of the reaction: AgCl(s) + 1/2 H2(g) = Ag(s) + HCl(aq), and the standard acidity constant of the ion HSO_4^- in synthetic seawater from 273.15 to 318.15 K. Journal of Chemical Thermodynamics 22, 113–127.

Domingues, R.B., Guerra, C.C., Barbosa, A.B., Galvãoa, H.M., 2017. Will nutrient and light limitation prevent eutrophication in an anthropogenically-impacted coastal lagoon? Continental Shelf Research 141, 11–25.

Edwards, R.J., van de Plassche, O., Gehrels, W.R., Wright, A.J., 2004. Assessing sea- level data from Connecticut, USA, using a foraminiferal transfer function for tide level. Marine Micropaleontology 51, 239–255.

Ellis, B.F., Messina, A., 1940. Catalogue of Foraminifera. Micropaleontology Press, New York. http://www.micropress.org.

Falcão, M., Vale, C., 1990. Study of the Ria Formosa ecosystem: benthic nutrient remineralization and total variability of nutrients in the water. Hydrobiologia 207, 137–146.

Fatela, F., Moreno, J., Leorri, E., Corbett, R., 2013. High marsh foraminiferal assemblages response to intra-decadal and multi-decadal precipitation variability, between 1934 and 2010 (Minho, NW Portugal). Journal of Sea Research. http://dx.doi.org/10. 1016/j.seares.2013.07.021.

Fatela, F., Moreno, J., Moreno, F., Araújo, M.F., Valente, T., Antunes, C., Taborda, R., Andrade, C., Drago, T., 2009. Environmental constraints of foraminiferal assemblages distribution across a brackish tidal marsh (Caminha, NW Portugal). Marine Micropaleontology 70, 70–88.

Flako-Zaritsky, S., Almogi-Labin, A., Schilman, B., Rosenfeld, A., Benjamini, C., 2011. The environmental setting and microfauna of the oligohaline Timsah pond, Israel: the last remnant of the Kabara swamps. Marine Micropaleontology 80, 74–88.

Francescangeli, F., Bouchet, V.M.P., Trentesaux, A., Armynot du Châtelet, E., 2017. Does elevation matter? Living foraminiferal distribution in a hyper tidal salt marsh (Canche Estuary, Northern France). Estuarine Coastal and Shelf Science 194, 192–204.

Gehrels, W.R., 1994. Determining relative sea level change from salt marsh foraminifera and plant zones on the coast of Maine, USA. Journal of Coastal Research 10, 990–1009.

Gehrels, W.R., Marshall, W.A., Gehrels, M.J., Larsen, G., Kirby, J.R., Eiriksson, J., Heinemeier, J., Shimmield, T., 2006. Rapid sea-level rise in the north Atlantic Ocean since the first half of the 19th century. The Holocene 16, 948–964.

Gehrels, W.R., Roe, H.M., Charman, D.J., 2001. Foraminifera, testate amoebae and diatoms as sea-level indicators in UK saltmarshes: a quantitative multiproxy approach. Journal of Quaternary Science 16, 201–220.

Grashoff, K., 1976. Methods of seawater analysis. Verlag Chemie, Weinheim, 317 pp.

Gustafsson, M., Nordberg, K., 1999. Benthic foraminifera and their response to hydrography, periodic hypoxic conditions and primary production in the Koljö fjord on the Swedish west coast. Journal of Sea Research 41, 163–178.

Hammer, Ø., Harper, D.A.T., Ryan, P.D., 2001. PAST. Paleontological statistics software package for education and data analysis. Palaeontologica Electronica 4, 9.

Haynert, K., Schönfeld, J., 2014. Impact of changing carbonate chemistry, temperature, and salinity on growth and test degradation of the benthic foraminifer *Ammonia aomoriensis*. Journal of Foraminiferal Research 44, 76–89.

Haynert, K., Schönfeld, J., Riebesell, U., Polovodova, I., 2011. Biometry and dissolution features of the benthic foraminifer *Ammonia aomoriensis* at high pCO_2. Marine Ecology Progress Series 432, 53–67.

Haynert, K., Schönfeld, J., Schiebel, R., Wilson, B., Thomsen, J., 2014. Response of benthic foraminifera to ocean acidification in their natural sediment environment: a long-term culturing experiment. Biogeosciences 11, 1581–1597.

Hayward, B.H., Figueira, B.O., Sabaa, A.T., Buzas, M.A., 2014. Multi-year life spans of high salt marsh agglutinated foraminifera from New Zealand. Marine Micropaleontology 109, 54–65.

Hayward, B.W., Grenfell, H.R., Scott, D.B., 1999. Tidal range of marsh foraminifera for determining former sea-level heights in New Zealand. New Zealand Journal of Geology and Geophysics 42, 395–413.

Hayward, B.W., Holzmann, M., Pawlowski, J., Parker, J.H., Kaushik, T., Toyofuku, M.S., Tsuchiya, M., 2021. Molecular and morphological taxonomy of living *Ammonia* and related taxa (Foraminifera) and their biogeography, Micropaleontology 67, 109–313.

Hayward, B.W., Scott, G.C., Grenfell, H.R., Carter, R., Lipps, J.H., 2004. Techniques for estimation of tidal elevation and confinement (~salinity) histories of sheltered harbours and estuaries using benthic foraminifera: examples from New Zealand. The Holocene 14, 218–232.

Heydemann, B., 1984. Das Ökosystem "Küsten-Salzwiese" - ein Überblick. Faunistisch- ökologische Mitteilungen 5, 249–279.

Horton, B., Murray, J., 2007. The roles of elevation and salinity as primary controls on living foraminiferal distributions: Cowpen Marsh, Tees Estuary, UK. Marine Micropaleontology 63, 169–186.

Horton, B.P., Edwards, R.J., 2006. Quantifying Holocene sea level change using intertidal foraminifera: lessons from the British Isles. Journal of Foraminiferal Research Special Publication 40, 1–97.

Horton, B.P., Edwards, R.J., Lloyd, J.M., 1999. A foraminiferal-based transfer function: implications for sea-level studies. Journal of Foraminiferal Research 29, 117–129.

Kaminski, M.A., Amao, A.O., Garrison, T.F., Fiorini, F., Magliveras, S., Tawabini, B.S., Waśkowska, A., 2020. An *Entzia*-dominated marsh-type agglutinated foraminiferal assemblage from a salt marsh in Tubli Bay, Bahrain. Geology, Geophysics & Environment 46, 189–204.

Katschnig, D., Broekman, R., Rozema, J., 2013. Salt tolerance in the halophyte *Salicornia dolichostachya* Moss: Growth, morphology and physiology. Environmental and Experimental Botany 92, 32–42.

Khanna, N., Godbold, J.A., Austin, W.E.N., Paterson, D.M., 2013. The Impact of Ocean Acidification on the Functional Morphology of Foraminifera. PLoS ONE 8, e83118, 4pp.

Koop-Jakobsen, K., Mueller, P., Meier, R.J., Liebsch, G., Jensen, K., 2018. Plant-sediment interactions in salt marshes – an optode imaging study of O_2, pH, and CO_2 gradients in the rhizosphere. Frontiers in Plant Science 9, 541, 11pp.

Koretsky, C.M., Van Cappellen, P., DiChristina, T.J., Kostka, J.E., Lowe, K.L., Moore, C.M., Roychoudhury, A.N., Viollier, E., 2005. Salt marsh pore water geochemistry does not correlate with microbial community structure. Estuarine, Coastal and Shelf Science 62, 233–251.

Korsun, S., Hald, M., Golikova, E., Yudina, A., Kuznetsov, I., Mikhailov, D., Knyazeva, O., 2014. Intertidal foraminiferal fauna and the distribution of elphidiidae at Chupa inlet, western White Sea. Marin Biology Research 10, 153–166.

Le Cadre, V., Debenay, J. P., Lesourd, M., 2003. Low pH effects on *Ammonia beccarii* test deformation: implications for using test deformations as a pollution indicator. Journal of Foraminiferal Research 33, 1–9.

Lehmann, G., 2000. Vorkommen, Populationsentwicklung, Ursache fleckenhafter Besiedlung und Fortpflanzungsbiologie von Foraminiferen in Salzwiesen und Flachwasser der Nord- und Ostseeküste Schleswig-Holsteins. Dissertation. University Kiel, Germany, 218 pp., http://macau.uni-kiel.de/receive/dissertation_ diss_413.

Leorri, E., Zimmerman, A.R., Mitra, S., Christian, R.R., Fatela, F., Mallinson, D., 2018. Refractory organic matter in salt marshes - effect on C sequestration calculations. Science of the Total Environment 633, 391–398.

Lewis, E., Wallace, D.W.R., 1998. Program Developed for CO2System Calculations, ORNL/CDIAC-105, Carbon Dioxide Information Analysis Center, Oak Ridge National Laboratory, U.S. Department of Energy, Oak Ridge, Tennessee, 38 pp.

Leyendekkers, J.V., 1973. The ionic activity function of water and the activity coefficient of the hydrogen ion in seawater. Limnology and Oceanography 18, 784–787.

Loureiro, S., Newton, A., Icely, J.D., 2006. Boundary conditions for the European Water Framework Directive in the Ria Formosa lagoon, Portugal (physico-chemical and phytoplankton quality elements). Estuarine Coastal and Shelf Science 67, 382–398.

Lübbers, J., Schönfeld, J., 2018. Recent saltmarsh foraminiferal assemblages from Iceland. Estuarine Coastal and Shelf Science 200, 380–394.

Lueker, T. J., Dickson, A.G., Keeling, C.D., 2000. Ocean pCO2 calculated from dissolved inorganic carbon, alkalinity, and equations for K1and K2: validation based on laboratory measurements of CO2 in gas and seawater at equilibrium. Marine Chemistry 70, 105–119.

Lutze, G.F., 1968. Jahresgang des Foraminiferen-Fauna in der Bottsand Lagune (westliche Ostsee). Meyniana 18, 13–30.

Mariotti, A., 2010. Recent changes in the Mediterranean water cycle: a pathway toward long-term regional hydroclimatic change? Journal of Climate 23, 1513–1525.

Mateu-Vicens, G., Box, A., Deudero, S., Beatriz Rodríguez, B., 2010. Comparative analysis of epiphytic foraminifera in sediments colonized by seagrass *Posidonia oceanica* and invasive macroalgae *Caulerpa* spp. Journal of Foraminiferal Research 40, 134–147.

McIntyre-Wressnig, A., Bernhard, J.M., McCorkle, D.C., Hallock, P., 2013. Non-lethal effects of ocean acidification on the symbiont-bearing benthic foraminifer *Amphistegina gibbosa*. Marine Ecology Progress Series 472, 45–60.

Melzner, F., Stange, P., Trübenbach, K., Thomsen, J., Casties, I., Panknin, U., Gutowska, M. A., 2011. Food supply and seawater pCO_2 impact calcification and internal shell dissolution in the blue mussel Mytilus edulis. Plos One 6, p. e24223.

Moreno, J., Fatela, F., Andrade, C., Cascalho, J., Moreno, F., Drago, T., 2005. Living Foraminiferal assemblages from Minho/Coura estuary (Northern Portugal): a stressfull environment. Thalassas 21, 17–28.

Moreno, J., Fatela, F., Leorri, E., Corbett, R., 2012. Caminha high marsh foraminifera response to precipitation: records from 1934 to 2010 of Minho region (NW Portugal). 7th Symposium on the Iberial Atlantic Margin, 16-20 December 2012, Lisbon, MIA12, 6pp.

Moreno, J., Valente, T., Moreno, F., Fatela, F., Guise, L., Patinha, C., 2007. Calcareous foraminifera occurrence and calcite-carbonate equilibrium conditions — a case study in Minho/Coura estuary (N Portugal). Hydrobiologia 597, 177–184.

Mouanga G.H., 2017. Impact and range extension of invasive foraminifera in the NW Mediterranean Sea: Implications for diversity and ecosystem functioning. Dissertation. Bonn University, Germany, 230 pp.

Müller-Navarra, K., Milker, Y., Schmiedl, G., 2016. Natural and anthropogenic influence on the distribution of salt marsh foraminifera in the Bay of Tümlau, German North Sea. Journal of Foraminiferal Research 46, 61–74.

Müller-Navarra, K., Milker, Y., Schmiedl, G., 2017. Applicability of transfer functions for relative sea-level reconstructions in the southern North Sea coastal region based on salt-marsh foraminifera. Marine Micropaleontology 135, 15–31.

Murray, J.W., 1971. Living foraminiferids of tidal marshes: a review. Journal of Foraminiferal Research 1, 153–161.

Murray, J., Alve, E. 2011. The distribution of agglutinated foraminifera in NW European seas: Baseline data for the interpretation of fossil assemblages. Palaeontologia Electronica 14.2.14A: 41 pp.

Murray, J.W., Sturrock, S., Weston, J.F., 1982. Suspended load transport of foraminiferal tests in a tide- and wave-swept sea. Journal of Foraminiferal Research 12, 51–65.

Muzavor, S., Pinto, J.R., Pinto, J.E., 2010. Roteiro ecológico da Ria Formosa, vol. 6, Flora. - Universidade do Algarve, CIMA - Centro de Investigação Marinha e Ambiental, Faro, Portugal, 74 pp.

Newton A., Mudge, S., 2005. Lagoon-sea exchanges, nutrient dynamics and water quality management of the Ria Formosa (Portugal). Estuarine, Coastal and Shelf Science 62, 405-414.

Nomaki, H., Heinz, P., Hemleben, C., Kitazato, H., 2005. Behavior and response of deep-sea benthic foraminifera to freshly supplied organic matter: a laboratory feeding experiment in microcosm environments. Journal of Foraminiferal Research 35, 103–113.

Oliveira, A.P., 1Cabeçadas, G., Mateus, M.D., 2017. Inorganic carbon distribution and CO_2 fluxes in a large European estuary (Tagus, Portugal). Scientific Reports 7, 7376, 14 pp.

Pacheco, A., Ferreira, O´., Williams, J.J., Garel, E., Vila-Concejo, A., Dias, J.A., 2010. Hydrodynamics and equilibrium of a multiple-inlet system. Marine Geology 274, 32–42.

Parker, F.L., Athearn, W.D., 1959. Ecology of marsh foraminifera in Poponesset Bay, Massachusetts. Journal of Paleontology 33, 333–343.

Páscoa, P., Gouveia, C.M., Russo, A., Trigo, R.M., 2017. Drought Trends in the Iberian Peninsula over the Last 112 Years. Advances in Meteorology 2017, 4653126, 13 pp.

Perez, F.F., Fraga, F., 1987. A precise and rapid analytical procedure for alkalinity determination. Marine Chemistry 21, 169–182.

Phleger, F.B., 1965a. Patterns of marsh foraminifera, Galveston bay, Texas. Limnology and Oceanography 10, 169–180.

Phleger, F.B., 1965b. Living foraminifera from a coastal marsh, southwestern Florida. Boletín de la Sociedad Geológica Mexicana, 28, 45–60.

Phleger, F.B., 1970. Foraminiferal populations and marine marsh processes. Limnology and Oceanography 15, 522–534.

Range, P., Chicharo, M.A., Ben-Hamadou, R., Piló, D., Matias, D., Joaquim, S., Oliveira, A.P., Chicharo, L., 2011. Calcification, growth and mortality of juvenile clams *Ruditapes decussatus* under increased pCO_2 and reduced pH: variable responses to ocean acidification at local scales? Journal of Experimental Marine Biology and Ecology 396, 177–184.

Range, P., Piló, D., Ben-Hamadou, R., Chícharo, M.A., Matias, D., Joaquim, S., Oliveira, A.P., Chícharo, L., 2012. Seawater acidification by CO_2 in a coastal lagoon environment: Effects on life history traits of juvenile mussels *Mytilus galloprovincialis*. Journal of Experimental Marine Biology and Ecology 424–425, 89–98.

Ranwell, D.S., 1972. Ecology of salt marshes and sand dunes. Chapman and Hall, London, 258 pp.

Reaves, C.M., 1986. Organic matter metabolizability and calcium carbonate dissolution in nearshore marine muds. Journal of Sedimentary Research 56, 486–494.

Ribas-Ribas, M., Anfuso, E., Gómez-Parra, A., Forja, J.M., 2013. Tidal and seasonal carbon and nutrient dynamics of the Guadalquivir estuary and the Bay of Cádiz (SW Iberian Peninsula). Biogeosciences, 10, 4481–4491.

Romanou A., Tselioudis G., Zerefos, C.S., Clayson, C.-A., Curry, J.A., Andersson, A., 2010. Evaporation–Precipitation Variability over the Mediterranean and the Black Seas from Satellite and Reanalysis Estimates. Journal of Climate 23, 5268–5287.

Rosa, A., Cardeira, S., Pereira, C., Rosa, M., Madureira, M., Rita, F., Jacob, J., Cravo, A., 2019. Temporal variability of the mass exchanges between the main inlet of Ria Formosa lagoon (southwestern Iberia) and the Atlantic Ocean. Estuarine Coastal and Shelf Science 228 (106349), 13 pp.

Rost, B., Riebesell, U. 2004. Coccolithophore calcification and the biological pump: response to environmental changes. In: Thierstein, H.R., Young, J.R. (Eds), Coccolithophores - From Molecular Processes to Global Impact. Springer, Berlin, pp. 99–125.

Rozema, J., Rozema-Dijst, E., Freijsen, A.H.J., Huber, J.J.L., 1978, Population differentiation within *Festuca rubra* L. with regard to soil salinity and soil water. Oecologia 34, 329–341.

Saderne, V., Fietzek, P., Herman, P.M.J., 2013. Extreme variations of pCO_2 and pH in a macrophyte meadow of the Baltic Sea in summer: evidence of the effect of photosynthesis and local upwelling. PLoS ONE 8, e62689, 8pp.

Sánchez, J.M., Izco, J., Medrano, M., 1996. Relationships between vegetation zonation and altitude in a salt-marsh system in northwest Spain. Journal of Vegetation Science 7, 695–702.

Saraswat, R., Kouthanker, M., Kurtarkar, S.R., Nigam, R., Naqvi, S.W.A., Linshy, V.N., 2015. Effect of salinity induced pH/alkalinity changes on benthic foraminifera: A laboratory culture experiment. Estuarine, Coastal and Shelf Science 153, 96–107.

Schönfeld, J., 2012. History and development of methods in Recent benthic foraminiferal studies. Journal of Micropalaeontology 31, 53–72.

Schönfeld, J., 2018. Monitoring benthic foraminiferal dynamics at Bottsand coastal lagoon (western Baltic Sea). Journal of Micropalaeontology 37, 383–393.

Schönfeld, J., Alve, E., Geslin, E., Jorissen, F., Korsun, S., Spezzaferri, S., 2012. The FOBIMO (FOraminiferal BIo-Monitoring) initiative e towards a standardised protocol for soft-bottom benthic foraminiferal monitoring studies. Marine Micropaleontology 94–95, 1–13.

Schönfeld, J., Beccari, V., Schmidt, S., Spezzaferri, S., 2021. Biometry and taxonomy of Adriatic Ammonia species from Bellaria–Igea Marina (Italy). Journal of Micropalaeontology 40, 195–223.
Schönfeld, J., Mendes, I., 2021. Environmental triggers of faunal changes revealed by benthic foraminiferal monitoring. Estuarine, Coastal and Shelf Science 253, 107313, 16 pp.
Schönfeld, J., Numberger, L., 2007. The benthic foraminiferal response to the 2004 spring bloom in the western Baltic Sea. Marine Micropaleontology 65, 78–95.
Scott, D.B., 1976. Quantitative studies of marsh foraminiferal patterns in the southern and their application to Holocene stratigraphic problems. Maritime Sediments, Special Publication 1, 153–170.
Scott, D.S., Medioli, F.S., 1978. Vertical zonations of marsh foraminifera as accurate indicators of former sea-levels. Nature 272, 528–531.
Scott, D.S., Medioli, F.S., 1980. Quantitative Studies of Marsh Foraminiferal Distributions in Nova Scotia: Implications for Sea Level Studies, Cushman Foundation for Foraminiferal Research, Special Publication 17, 1–58.
Seeberg-Elverfeldt, J., Schlüter, M., Feseker, T., and Kölling, M., 2005. A Rhizon in situ sampler (RISS) for pore water sampling from aquatic sediments. Limnology Oceanography Methods 3, 361–371.
Silva, H., Caldeira, G., Freitas, H., 2007. *Salicornia ramosissima* population dynamics and tolerance of salinity. Ecological Research 22, 125–134.
Silvestri, S., Defina, A., Marani, M., 2005. Tidal regime, salinity and salt marsh plant zonation. Estuarine, Coastal and Shelf Science 62, 119–130.
Stigter, T.Y., van Ooijen, S.P.J., Post, V.E.A., Appelo, C.A.J, de Carvalho Dill, A.M.M., 1998. A hydrogeological and hydrochemical explanation of the groundwater composition under irrigated land in a Mediterranean environment, Algarve. Journal of Hydrology 208, 262–279.
Suchrow, S., 2014. Modelling spatial and temporal patterns of surface elevation and vegetation in German North Sea salt marshes. Dissertation, Hamburg University, Germany, 215 pp.
Suchrow, S., Jensen, K., 2010. Plant species responses to an elevational gradient in German North Sea salt marshes. Wetlands 30, 735–746.
Tett, P., Gilpin, L., Svendsen, H., Erlandsson, C.P., Larsson, U., Kratzer, S., Fouilland, E., Janzen, C., Lee, J.-Y., Grenz, C., Newton, A., Ferreira, J.G., Fernandes, T., Scory, S., 2003. Eutrophication and some European waters of restricted exchange. Continental Shelf Research 23, 1635–1671.
Thomas, H., Schiettecatte, L.S., Suykens, K., Koné, Y.J.M., Shadwick, E.H., Prowe, A.E.F., Bozec, Y., de Baar, H.J.W., Borges, A.V., 2009. Enhanced ocean carbon storage from anaerobic alkalinity generation in coastal sediments. Biogeosciences 6, 267–274.
Valente, T., Fatela, F., Moreno, J., Moreno, F., Guise, L., Patinha, C., 2009. A comparative study of the influence of geochemical parameters on the distribution of foraminiferal assemblages in two distinctive tidal marshes. Journal of Coastal Research, SI 56, 1439–1443.
Van Hengstum, P.J., Scott, D.B., 2011. Ecology of foraminifera and habitat variability in an underwater cave: distinguishing anchialine versus submarine cave environments. Journal of Foraminiferal Research 41, 201–229.
Vogel, N., Uthicke, S., 2012. Calcification and photobiology in symbiont-bearing benthic foraminifera and responses to a high CO_2 environment. Journal of Experimental Marine Biology and Ecology 424–425, 15–24.
Wang, F., Kroeger, K.D., Gonneea, M.E., Pohlman, J.W., Tang, J., 2019. Water salinity and inundation control soil carbon decomposition during salt marsh restoration: An incubation experiment. Ecology and Evolution 9, 1911–1921.
Wang, Z.A., Kroeger, K.D., Ganju, N.K., Gonneea, M.E., Chu, S.N., 2016. Intertidal salt marshes as an important source of inorganic carbon to the coastal ocean. Limnology and Oceanography 61, 1916–1931.
WoRMS Editorial Board, 2022. World register of marine species. http://www.marinespecies.org.

Supplements

Supplement Fig. 1. Preservation stages of *Ammonia aberdoveyensis.*
Supplement Fig. 2. Temperatures and salinities in Esteiro do Ancão.
Supplement Fig. 3. Inundation time as proportion of one lunar year.
Supplement Table 1. Hydrogen ion activity coefficients in seawater.
Supplement Table 2. Sediment properties, salt marsh flora, and macroorganisms at the transect.

Supplement Table 3. Temperature and salinity measurements at Ria Formosa and Gulf of Cadiz.
Supplement Table 4. Temperature, salinity, pH and alkalinity measurements of pore and surface water samples, and carbonate sytem parameters.
Supplement Table 5. Foraminiferal census data from 2018.
Supplement Table 6. Foraminiferal census data from 2019.
Supplement Table 7. Faunal and environmental parameters.

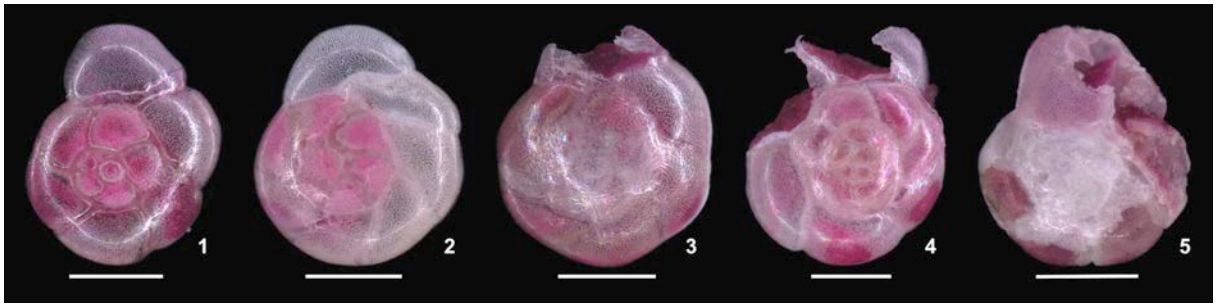

Supplement Fig. 1. Preservation stages of *Ammonia aberdoveyensis*. Stage 1 = glossy test (sample 208), Stage 2 = dull shell wall (sample 198), Stage 3 = dissolution or loss of the last chamber (sample 198), Stage 4 = dissolution of more chambers (sample 197), Stage 5 = almost complete dissolution of the outer chamber wall (sample 214). Scale bar = 100 µm.

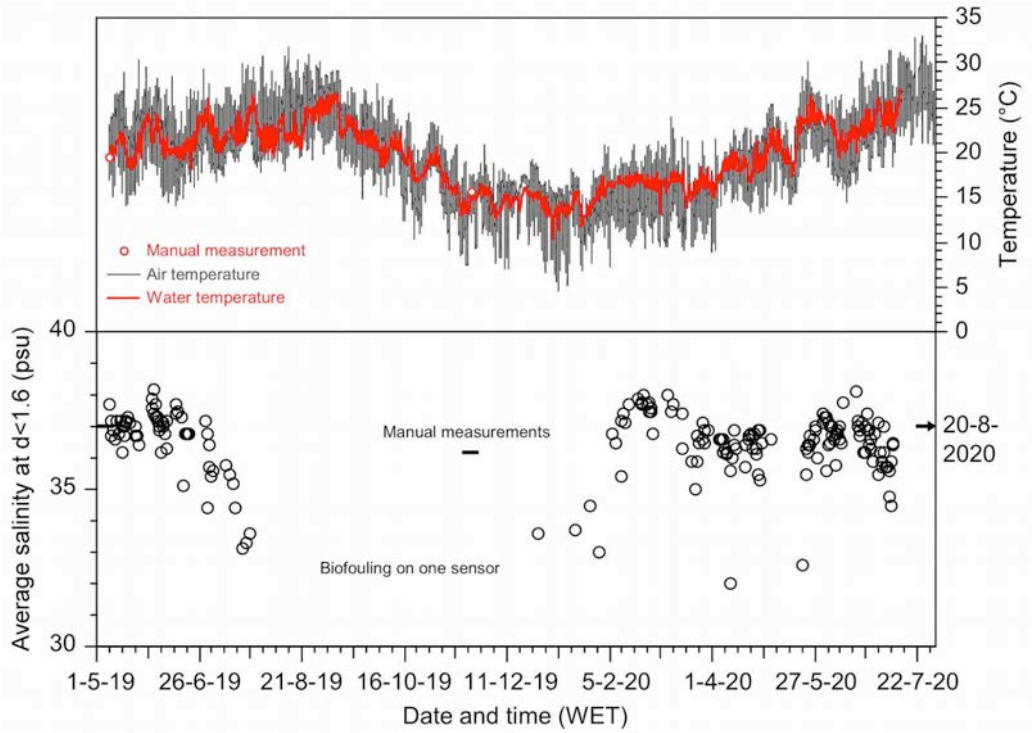

Supplement Fig. 2. Temperatures and salinities in Esteiro do Ancão measured at the hydrographic monitoring station. Abbreviations: d: difference between individual sensor readings, WET: Western European Time.

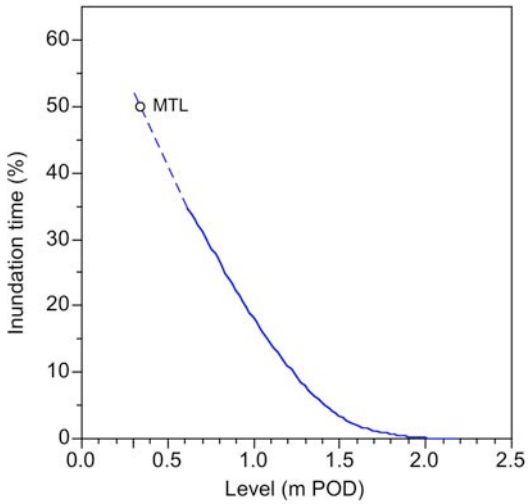

Supplement Fig. 3. Inundation time as proportion of the one lunar year observation period. Dashed line: approximation for levels between the sensor hight (0.61 m POD) and the vegetation boundary. Abbreviation: MTL: Mean Tidal Level (0.34 m POD).

Supplement Table 1. Hydrogen ion activity coefficients in seawater. Interpolated from values provided by Leyendekkers (1973).

Salinity measured	diluted 11:10	Temperature (°C) 0	10	11	12	13	14	15	16	17	18	19	20	21	22	23	24	25
27.1	**24.6**	**0.767**	0.750	0.748	0.746	0.745	0.743	0.742	0.740	0.739	0.737	0.736	0.734	0.733	0.731	0.730	0.728	**0.727**
28.6	26	0.769	0.752	0.751	0.749	0.747	0.746	0.744	0.743	0.741	0.739	0.738	0.736	0.735	0.733	0.731	0.730	0.729
29.7	27	0.770	0.754	0.753	0.751	0.750	0.748	0.747	0.745	0.743	0.742	0.740	0.739	0.737	0.736	0.734	0.732	0.730
30.8	28	0.772	0.756	0.754	0.753	0.751	0.749	0.748	0.746	0.744	0.743	0.741	0.740	0.738	0.736	0.735	0.733	0.731
31.9	29	0.773	0.757	0.756	0.754	0.752	0.751	0.749	0.747	0.746	0.744	0.742	0.741	0.739	0.737	0.736	0.734	0.733
33.0	30	0.775	0.759	0.757	0.756	0.754	0.752	0.751	0.749	0.747	0.746	0.744	0.742	0.740	0.739	0.737	0.735	0.734
34.1	31	0.777	0.762	0.760	0.758	0.757	0.755	0.753	0.752	0.750	0.748	0.747	0.745	0.743	0.741	0.740	0.738	0.736
35.2	32	0.779	0.764	0.762	0.760	0.759	0.757	0.755	0.753	0.752	0.750	0.748	0.747	0.745	0.743	0.741	0.739	0.737
36.3	33	0.781	0.766	0.764	0.762	0.761	0.759	0.757	0.756	0.754	0.752	0.750	0.749	0.747	0.745	0.743	0.741	0.739
37.5	**34.1**	**0.784**	0.768	0.766	0.765	0.763	0.761	0.760	0.758	0.756	0.754	0.753	0.751	0.749	0.747	0.745	0.743	**0.741**
38.5	35	0.786	0.771	0.769	0.767	0.765	0.764	0.762	0.760	0.758	0.757	0.755	0.753	0.751	0.749	0.747	0.746	0.743
39.6	36	0.789	0.772	0.771	0.769	0.767	0.765	0.764	0.762	0.760	0.758	0.756	0.754	0.752	0.751	0.749	0.747	0.745
40.7	37	0.792	0.775	0.773	0.772	0.770	0.768	0.766	0.765	0.763	0.761	0.759	0.757	0.755	0.753	0.751	0.749	0.748
41.8	38	0.795	0.778	0.776	0.775	0.773	0.771	0.769	0.767	0.765	0.764	0.762	0.760	0.758	0.756	0.754	0.752	0.750
42.9	39	0.798	0.781	0.780	0.778	0.776	0.774	0.772	0.770	0.769	0.767	0.765	0.763	0.761	0.759	0.757	0.755	0.753
44.0	40	0.801	0.784	0.782	0.780	0.778	0.776	0.774	0.772	0.770	0.769	0.767	0.765	0.763	0.761	0.759	0.757	0.755
45.1	41	0.805	0.787	0.785	0.783	0.782	0.780	0.778	0.776	0.774	0.772	0.770	0.768	0.766	0.764	0.762	0.760	0.758
46.2	42	0.808	0.790	0.788	0.786	0.784	0.782	0.780	0.778	0.776	0.774	0.772	0.770	0.768	0.766	0.764	0.762	0.761
47.3	43	0.812	0.794	0.792	0.790	0.788	0.786	0.784	0.782	0.780	0.778	0.776	0.774	0.772	0.770	0.768	0.766	0.764
48.4	44	0.816	0.797	0.795	0.793	0.791	0.789	0.787	0.785	0.783	0.781	0.779	0.777	0.775	0.773	0.771	0.769	0.767
49.5	45	0.820	0.800	0.798	0.796	0.794	0.792	0.790	0.788	0.786	0.784	0.782	0.780	0.778	0.776	0.774	0.772	0.770
50.6	46	0.824	0.804	0.802	0.800	0.798	0.796	0.794	0.792	0.790	0.788	0.786	0.784	0.782	0.780	0.778	0.776	0.774
51.7	47	0.829	0.808	0.806	0.804	0.802	0.800	0.797	0.795	0.793	0.791	0.789	0.787	0.785	0.783	0.781	0.779	0.777
52.8	**48**	**0.833**	0.812	0.810	0.808	0.806	0.804	0.802	0.800	0.797	0.795	0.793	0.791	0.789	0.787	0.785	0.783	**0.781**

Salinity measured	diluted 11:10	Temperature (°C) 25	26	27	28	29	30	31	32	33	34	35	36	37	38	39	40
27.1	**24.6**	**0.727**	0.725	0.724	0.722	0.721	0.720	0.718	0.718	0.717	0.715	0.714	0.713	0.712	0.710	0.709	**0.707**
28.6	26	0.729	0.727	0.725	0.724	0.722	0.721	0.719	0.719	0.717	0.716	0.715	0.713	0.712	0.710	0.709	0.707
29.7	27	0.730	0.729	0.728	0.726	0.725	0.723	0.722	0.718	0.717	0.715	0.714	0.712	0.710	0.709	0.707	0.707
30.8	28	0.731	0.730	0.728	0.727	0.725	0.723	0.722	0.719	0.718	0.716	0.714	0.713	0.711	0.709	0.708	0.707
31.9	29	0.733	0.731	0.729	0.727	0.726	0.724	0.722	0.720	0.718	0.717	0.715	0.713	0.711	0.710	0.708	0.707
33.0	30	0.734	0.732	0.730	0.728	0.727	0.725	0.723	0.722	0.720	0.718	0.717	0.715	0.713	0.712	0.710	0.707
34.1	31	0.736	0.734	0.732	0.731	0.729	0.727	0.725	0.723	0.721	0.719	0.717	0.715	0.713	0.711	0.709	0.708
35.2	32	0.737	0.736	0.734	0.732	0.730	0.728	0.726	0.725	0.723	0.721	0.719	0.718	0.716	0.714	0.712	0.709
36.3	33	0.739	0.738	0.736	0.734	0.732	0.730	0.728	0.726	0.724	0.722	0.720	0.718	0.716	0.714	0.712	0.710
37.5	**34.1**	**0.741**	0.740	0.738	0.736	0.734	0.732	0.730	0.728	0.726	0.724	0.722	0.720	0.718	0.715	0.713	**0.711**
38.5	35	0.743	0.742	0.740	0.738	0.736	0.734	0.732	0.729	0.727	0.725	0.723	0.721	0.719	0.716	0.714	0.713
39.6	36	0.745	0.743	0.741	0.739	0.737	0.735	0.733	0.731	0.729	0.727	0.725	0.722	0.720	0.718	0.716	0.714
40.7	37	0.748	0.746	0.744	0.742	0.740	0.738	0.736	0.732	0.730	0.728	0.726	0.724	0.722	0.719	0.717	0.716
41.8	38	0.750	0.748	0.746	0.744	0.742	0.740	0.738	0.736	0.733	0.731	0.729	0.727	0.725	0.723	0.720	0.718
42.9	39	0.753	0.751	0.749	0.747	0.745	0.743	0.741	0.738	0.735	0.733	0.731	0.729	0.726	0.724	0.722	0.721
44.0	40	0.755	0.752	0.750	0.748	0.746	0.744	0.742	0.741	0.739	0.737	0.735	0.733	0.730	0.728	0.726	0.723
45.1	41	0.758	0.756	0.754	0.752	0.750	0.748	0.745	0.743	0.741	0.739	0.737	0.735	0.732	0.730	0.728	0.726
46.2	42	0.761	0.758	0.756	0.754	0.752	0.749	0.747	0.747	0.745	0.743	0.741	0.739	0.737	0.735	0.732	0.729
47.3	43	0.764	0.762	0.760	0.758	0.756	0.753	0.751	0.749	0.747	0.745	0.743	0.741	0.738	0.736	0.734	0.732
48.4	44	0.767	0.765	0.763	0.761	0.759	0.757	0.754	0.752	0.750	0.748	0.746	0.744	0.742	0.740	0.737	0.735
49.5	45	0.770	0.768	0.766	0.764	0.762	0.760	0.758	0.756	0.754	0.751	0.749	0.747	0.745	0.743	0.741	0.739
50.6	46	0.774	0.771	0.769	0.767	0.765	0.763	0.761	0.759	0.757	0.755	0.753	0.751	0.749	0.747	0.745	0.743
51.7	47	0.777	0.775	0.773	0.771	0.769	0.767	0.765	0.763	0.761	0.759	0.757	0.755	0.753	0.751	0.749	0.747
52.8	**48**	**0.781**	0.779	0.777	0.775	0.773	0.771	0.769	0.765	0.763	0.761	0.759	0.757	0.755	0.753	0.751	**0.751**

bold: measured values from Leyendekkers, J.V., 1973. The ionic activity function of water and the activity coefficient of the hydrogen ion in seawater. Limnology and Oceanography 18, 784-787: there Table 1.

Supplement Table 2. Observations of sediment properties, structures, salt marsh flora, and macroorganisms occurrences along the western Ria Formosa salt marsh transect. Distances are given in meters from transect zero.

5-May-2018	6-May-2019
(0) - 1.5 m: medium to coarse sand with shell debris, surface even, covered by a mat of rotten *Zostera noltii* leaves, single *Arthrocnemum macrostachyum* in patches, low *Suaeda vera* sporadically.	(0) - 5.0 m: coarse sand with shell debris, surface even, covered with a 3 cm thick filz of rotten *Zostera* debris. The leaves are whitish-bleached on the top and dark-brown at deeper levels. Vegetation: 0.5 - 1.75 m high and strong *Arthrocnemum macrostachyum*,
1.5 - 2.9 m: humus-rich mud, 2 cm thick, above medium to coarse sand, surface even, covered by a mat of *Zostera noltii* debris, no vegetation (foot path).	1.75 - 2.75 m: foot path with no vegetation,
2.9 - 5.2 m: mud rich in rotten plant debris, 5 cm thick, above coarse sand, surface even, dense and homogenously vegetated with ca. 60 cm high *Arthrocnemum macrostachyum*.	2.75 - 5.9 m: high, dense and strong *Arthrocnemum macrostachyum*.
5.2 - 7.9 m: soft, clayey, humus-rich mud with rotten plant debris, 5 cm thick, above sand, surface covered by a thin mat of *Zostera* and *Juncus* leaves, and filamentous green algae (*Enteromorpha*), single bivalve shells, vegetated with high *Arthrocnemum macrostachyum*.	5.0 - 7.4 m: mat of rotten plant debris of *Zostera* and *Juncus* leaves, and crab shells, 3 cm thick, above muddy sand with black and brown spots.
7.9 - 21.3 m: humus-rich mud, surface even, dense and homogenously vegetated with low *Arthrocnemum macrostachyum*. First *Halimione portulacoides* at 18.4 m (upper-lower salt marsh boundary), first, scattered *Sparitima maritima* at 19.0 m.	7.4 - 14.6 m: organic-rich olive-brown mud, surface even, covered with plant debris of *Zostera* and *Juncus* leaves, vegetated with low and dense *Arthrocnemum macrostachyum*.
21.3 - 25.8 m: humus-rich mud, grey with dark-brown spots, surface even, densely vegetated with high *Arthrocnemum macrostachyum*. *Halimione portulacoides* was common and homogenously distributed. Debris seam of *Zostera* and *Juncus* leaves on the plants.	14.6 - 25.7 m: soft organic-rich mud stabilized by a dense root network, vegetated with high and low *Arthrocnemum macrostachyum*. A single *Halimione portulacoides* at 17.6 m south, and at 18.6 m on the transect (upper-lower salt marsh boundary), first, isolated *Sparitima maritima* at 20.1 m, *Halimione portulacoides* was common from 23.7 m.
25.8 - 30.3 m: soft mud, grey or brown coloured, surface even, very densely vegetated with low, creeping *Arthrocnemum macrostachyum* and scattered *Halimione portulacoides*. Single *Spartina maritima* from 26.2 m, a marked patch of *Limonium vulgare* south of the transect between 26.8 and 27.8 m.	25.7 - 30.6 m: soft, plastic light-brown mud, surface flat, vegetated with low and dense *Arthrocnemum macrostachyum* and few *Halimione portulacoides* extending until 29.9 m, few scattered *Spartina maritima*, a patch of *Limonium vulgare* 2 - 3 m south of the transect, between 26.8 and 27.7 m.

Supplement Table 2 (continuation).

5-May-2018	6-May-2019
30.3 - 47.5 m: soft mud, black and anoxic a few mm below uneven surface, covered by a patchy mat of *Enteromorpha* and *Fucus vesiculosus*. Dense vegetation of *Spartina maritima* (lower salt marsh - pioneer zone boundary), a few runners of *Arthrocnemum macrostachyum* up to 31.3 m. Small tidal pond between 32 and 33.2 m.	30.6 - 47.2 m: soft, clayey mud with brown and black spots, surface undulated, covered with rotten *Enteromorpha* and *Fucus vesiculosus*, vegetated by low and dense *Spartina maritima* (lower salt marsh - pioneer zone boundary). Tidal pond between 32 and 33.2 m.
47.5 - 51.4 m (vegetation boundary): muddy coarse sand with bivalve shells and few pebbles, black and anoxic a few mm below hummocky surface, fiddler crab burrows common. Loose vegetation of low *Spartina maritima*, few Enteromorpha.	47.2 - 51.9 m (vegetation boundary): sandy mud passing into muddy, coarse sand with black and brown dots at depth. Surface irregularly undulated, with single and double bivalve shells. Fiddler crab burrows frequent. Less dense vegetation of low *Spartina maritima*.
51.4 - 58.2 m: muddy coarse sand with shell debris and few small pebbles, black and anoxic 1 cm below uneven surface, fiddler crab burrows frequent, openings of polycheat tubes 1-2 mm diameter common. *Littorina* in puddles, sparse *Zostera noltii* from 54.2 m.	51.9 - 55.1 m: coarse sand with bivalve shells above muddy sand, with a distinct colour change from greyish-brown to black at 5 mm below surface. Surface undulated. Large fiddler crab burrows common and ca. 0.4 m apart to each other. Abundant openings of polychaete tubes of 3 - 5 mm diameter. Few, brown *Zostera noltii* leaves on the surface.
	55.1 - 56.5 m: muddy sand, surface undulated with more gastropod than bivalve shells, clear redox boundary at 5 mm below surface, vegetated by a few, scattered *Zostera noltii*.
58.2 - 77.5 m: sandy mud, black and anoxic a few mm below even surface, vegetated with *Zostera noltii*.	56.5 - 60.2 m: sandy mud, surface undulated with gastropod and bivalve shells, redox boundary at 5 mm below surface, vegetated by *Zostera noltii*.
	60.2 - 68.5 m: soft mud of 10 cm thickness above sandy mud. *Zostera noltii* abundant.
77.5 - 87.0 m: soft, clayey mud, surface even, scattered bivalve shells on the surface, densely vegetated with *Zostera noltii*.	68.5 - 88.2 m: sticky soft mud, redox boundary a few millimetres below surface, few double bivalve shells on the surface, vegetated by dense and homogenous *Zostera noltii*, patches of *Enteromorpha*, few *Ulva* in places. A reed post overgrown with barnacles at 82.3 m.
87.0 - 88 m: clayey, sandy mud with bivalve and gastropod shell debris, vegetated with *Zostera noltii*.	
88 - 90 m (tidal channel): gastropod and bivalve shell-rich sandy mud, dense and patchy vegetated with *Zostera noltii*. Small hermit crabs common.	88.2 - 90 m (tidal channel): muddy sand with abundant shells on the surface, anoxic at depth, vegetated by loose *Zostera noltii*. Large shore crabs, hermit crabs, gastropods, and small brown sea slugs resting on *Zostera* leaves.
90 - (94 m): very soft clayey mud, surface even with few bivalve shells, densely vegetated with *Zostera noltii*. Concrete post overgrown with oysters and barnacles at 94 m.	

Supplement Table 3. Temperature and salinity measurements of Ria Formosa and Gulf of Cadiz surface water.

Year	Date	Time	Tide	Location	Instrument	Temperature (°C)	Salinity
2018	04.05.18	10:05	ebb	Ponte da Praia de Faro	Cond3210	18.0	36.3
	04.05.18	10:25	ebb	Praia de Faro	Cond3210	17.3	36.0
	06.05.18	12:20	ebb	Ponte da Praia de Faro	Cond3210	21.0	36.1
	06.05.18	12:45	ebb	Praia de Faro	Cond3210	18.4	36.0
	07.05.18	09:28	ebb	Salt marsh transect, 48 m	Cond3210	21.6	36.4
	08.05.18	12:35	ebb	Ponte da Praia de Faro	Cond3210	21.8	36.2
	08.05.18	12:52	ebb	Praia de Faro	Cond3210	18.0	36.1
2019	02.05.19	07:40	ebb	Ponte da Praia de Faro	LF320	21.6	37.0
	02.05.19	08:00	ebb	Praia de Faro	LF320	18.1	36.0
	03.05.19	18:17	ebb	Salt marsh transect, 50 m	LF320	25.2	37.0
	05.05.19	08:20	ebb	Ponte da Praia de Faro	LF320	20.9	37.0
	05.05.19	08:45	ebb	Praia de Faro	LF320	18.3	36.1
	05.05.19	10:03	ebb	Salt marsh transect, 89 m	LF320	25.7	37.6
	07.05.19	10:20	ebb	Ponte da Praia de Faro	LF320	19.4	37.1
	07.05.19	09:55	ebb	Praia de Faro	LF320	17.4	36.0
	09.05.19	11:55	ebb	Ponte da Praia de Faro	LF320	20.5	37.0
	09.05.19	12:10	ebb	Praia de Faro	LF320	18.0	36.0
2019	29.11.19	09:00	ebb	Ponte da Praia de Faro	LF320	15.4	36.3
	29.11.19	09:00	ebb	Ponte da Praia de Faro	LF320	15.7	36.0
	29.11.19	09:00	ebb	Ponte da Praia de Faro	LF320	15.4	36.2
2020	20.08.20	14:50	flood	Mid of boardwalk to Ponte	LF320	25.8	37.3
	20.08.20	15:10	flood	Mid of boardwalk to Ponte	LF320	25.1	37.2
	20.08.20	15:30	flood	Mid of boardwalk to Ponte	LF320	24.0	37.1
	20.08.20	15:50	flood	Mid of boardwalk to Ponte	LF320	23.3	37.0
	20.08.20	16:10	flood	Mid of boardwalk to Ponte	LF320	22.9	37.0
	20.08.20	16:30	flood	Mid of boardwalk to Ponte	LF320	24.1	37.0
	20.08.20	17:40	ebb	Mid of boardwalk to Ponte	LF320	23.3	36.9
	20.08.20	18:00	ebb	Mid of boardwalk to Ponte	LF320	23.1	36.9
	20.08.20	18:20	ebb	Mid of boardwalk to Ponte	LF320	22.6	36.6
	20.08.20	18:40	ebb	Mid of boardwalk to Ponte	LF320	22.9	36.7
					Minimum (May):	17.3	36.0
					Maximum (May):	25.7	37.6
					Mean value (May):	20.1	36.5
					Mean salt marsh transect (May):	24.2	37.0
					Mean Esteiro do Ancão (May):	20.5	36.7
					Mean Gulf of Cadiz (May):	17.9	36.0
					Mean Esteiro do Ancão (August):	23.7	37.0
					Mean Esteiro do Ancão (November):	15.5	36.2

Supplement Table 4. Temperature, salinity, pH and alkalinity measurements of pore and surface water samples, and carbonate sytem parameters calculated with co2sys_ver25b06.xls.

Date	Location, Station	Sample	Section m	Sediment temp. (°C)	Water temp. (°C)	Salinity	ph (NIST)	Alkalinity (µmol kg^{-1})	$[CO_3^{-}]$ (µmol kg^{-1})	pCO_2 (µatm)	Ω Ca
a) Pore water samples											
7.5.18	191		3	32.8	31.0	48.3	7.076	2203.6	32.97	6455	0.70
7.5.18	192		7	34.0	31.7	36.5	6.898	2224.9	18.14	10187	0.44
7.5.18	193	a	15	35.0	32.4	40.8	6.646	2219.7	11.29	18148	0.26
7.5.18	193	b	15	31.3	31.2	41.9	6.280	2212.9	4.76	41504	0.11
7.5.18	194		22	30.2	29.5	38.5	6.369	2189.4	5.05	32918	0.12
7.5.18	195		25	31.9	32.2	38.9	6.373	2218.6	5.61	33919	0.13
7.5.18	196		29	32.8	32.4	37.1	6.578	2220.5	8.7	21274	0.21
7.5.18	197		37	29.1	29.7	39.3	6.148	1924.1	2.68	47875	0.06
7.5.18	198		48	32.5	32.4	40.5	6.438	2216.5	6.95	29389	0.16
7.5.18	199		52.5	29.8	29.6	38.2	7.545	2215.7	70.43	2061	1.66
7.5.18	200		56.1	29.2	29.4	38.5	7.077	2215.7	25.14	6336	0.59
7.5.18	201		61.5	31.0	31.3	39.5	7.476	2162.8	64.24	2412	1.50
7.5.18	202		72.6	31.4	31.0	37.4	6.990	2219.2	21.62	8014	0.52
3.5.19	207	a	3	19.4	20.5	49.6	7.081	2185.0	24.5	5552	0.51
3.5.19	207	b	3	19.4	20.8	47.3	7.427	2187.1	50.5	2423	1.08
3.5.19	208	a	7	20.0	20.6	42.6	7.058	2205.5	20.7	5997	0.47
3.5.19	208	b	7	20.0	21.1	41.6	7.384	2206.6	41.6	2758	0.94
3.5.19	209	a	15	21.7	27.1	40.4	7.686	2207.7	80.3	1336	1.84
3.5.19	209	b	15	21.7	22.0	43.9	6.331	2190.5	4.2	32746	0.09
3.5.19	209	b (rept.)	15	21.7	22.4	43.9	6.331	2192.3	4.2	32773	0.09
3.5.19	210	a	22	23.5	23.1	44.7	6.566	2201.7	7.9	19642	0.17
3.5.19	210	b	22	23.5	22.8	46.5	6.435	2197.9	6.1	26622	0.13
4.5.19	210	a	22	21.7	26.1	48.5	5.911	2116.6	1.9	87804	0.04
4.5.19	210	b	22	21.7	25.6	44.5	6.344	2199.5	4.9	33372	0.11
4.5.19	211	a	25	17.7	20.8	44.9	6.562	2196.9	6.8	18690	0.15
4.5.19	211	b	25	17.7	21.1	47.3	6.486	2192.9	6.1	22355	0.13
4.5.19	212	a	29	18.2	20.0	42.0	6.814	2203.1	10.9	10333	0.25
4.5.19	212	b	29	18.2	20.3	41.8	6.944	2205.6	15.1	7743	0.34
4.5.19	213	a	37	19.9	22.6	39.3	6.633	2207.5	7.4	16390	0.17
4.5.19	213	b	37	19.9	22.9	39.1	6.812	2208.4	11.2	10858	0.26
4.5.19	214	a	48	21.8	25.1	39.1	6.695	2207.5	9.6	14857	0.22
4.5.19	214	b	48	21.8	24.8	38.3	6.557	2212.1	6.8	20469	0.16
4.5.19	215	a	52	23.9	25.1	37.9	6.907	2214.9	14.8	9059	0.35
4.5.19	215	b	52	23.9	24.5	38.6	6.926	2213.6	15.7	8634	0.37
4.5.19	216	a	56	24.5	24.3	38.0	7.308	2212.1	35.2	3465	0.82
4.5.19	216	b	56	24.5	24.4	37.8	7.372	2214.7	41.4	2999	0.97
5.5.19	217	a	61.5	25.8	18.1	37.6	7.340	2215.4	35.8	3168	0.84
5.5.19	217	b	61.5	25.8	22.0	37.8	6.959	2207.7	13.2	7369	0.31
5.5.19	218	a	72.6	25.1	23.3	38.3	6.892	2214.6	13.1	9036	0.31
5.5.19	218	b	72.6	25.1	23.2	39.1	7.016	2212.8	16.0	6517	0.37
5.5.19	219	a	81	23.7	22.4	37.7	7.148	2214.9	22.9	4960	0.54
5.5.19	219	b	81	23.7	22.4	37.5	7.213	2214.6	26.8	4291	0.63
5.5.19	220	a	87.1	23.1	21.2	37.2	7.394	2198.5	39.4	2760	0.93
5.5.19	220	b	87.1	23.1	22.3	37.2	7.728	2204.8	77.3	1204	1.82
b) Surface water samples											
7.5.18	198		48		26.3	36.4	7.879	2211.3	122.7	865	2.92
3.5.19	214		50		25.2	37.0	8.277	2208.5	243.5	282	5.76
5.5.19	221		89		25.7	37.6	8.576	2212.3	359.6	111	8.43
5.5.19	Ponte				20.9	37.0	8.111	2206.8	162.0	443	3.81
7.5.19	Ponte	a*			19.4	37.1	8.053	2207.7	163.5	531	3.86
7.5.19	Ponte	b*			19.4	37.1	8.055	2207.4	165.4	529	3.91
7.5.19	Ponte	c*			19.4	37.1	8.058	2207.4	165.9	525	3.92
8.5.18	Ponte	a			24.8	36.2	8.104	2208.7	180.3	468	4.30
8.5.18	Ponte	b			24.8	36.2	8.120	2208.5	185.6	448	4.42
8.5.18	Ponte	c			24.1	36.2	8.126	2208.7	184.4	439	4.39
8.5.18	Ponte	d			24.6	36.2	8.125	2209.4	186.5	441	4.44
5.5.19	Praia				18.3	36.1	8.084	2174.6	149.2	472	3.54
7.5.19	Praia	a*			17.4	36.0	8.041	2180.4	155.2	548	3.70
7.5.19	Praia	b*			17.4	36.0	8.041	2177.5	155.0	547	3.70
7.5.19	Praia	c*			17.4	36.0	8.042	2177.4	154.9	546	3.69
8.5.18	Praia	a			24.9	36.1	8.010	2167.4	148.5	594	3.54
8.5.18	Praia	b			24.6	36.1	8.062	2171.7	163.0	515	3.89
8.5.18	Praia	c			25.2	36.1	8.061	2161.3	164.4	516	3.92
				Mean Esteiro do Ancão:		36.7	8.135	2208.8	192.7	462.0	4.6
				Mean Gulf of Cadiz:		36.1	8.049	2172.9	155.8	534.1	3.7

* indoor measurements, rept.: repetition of the same sample, Ponte: Esteiro do Ancão ebb water, Praia: Gulf of Cadiz water

Supplement Table 5. Foraminiferal census data 2018, Ria Formosa salt marsh transect.

Sampling date: 5-May-2018																
Counted specimens	Sample:	190	191	192	193	194	195	196	197	198	199	200	201	202	203	204	205
	Section m:	0.0	3.0	7.0	15.0	22.0	25.0	29.0	37.0	48.0	52.2	56.1	61.5	72.6	81.0	87.1	89.0
Species	Hight (m POD):	1.63	1.48	1.36	1.25	1.20	1.20	0.95	0.80	0.50	0.28	0.19	0.08	-0.12	-0.24	-0.34	-0.48
Affinetrina planciana			2	6					3	14	1	4	2				
Ammonia aberdoveyensis		21	34	11		8	13		57	76							
Ammonia advena						1											
Ammonia batava								5									
Ammonia tepida											7	13	10		2	24	5
Ammoscalaria runiana												9	3	4		8	1
Ammotium salsum				1						1		3	1				2
Arenoparrella mexicana								2		1							
Asterigerinata mamilla												1	1		1	1	
Aubignyna hamblensis											6	3	23	2	14	6	1
Bisaccium imbricatum												1					
Bolivina ordinaria										1	2				7		1
Bolivina striatula								1			1	4	6		1		1
Buccella granulata										1		9	1	1			
Cornuspira involvens		1						2		3	3	4	2				
Crithionina granum					1	2		1		1							
Crithionina mamilla											1					1	3
Eggerella europea									2								
Elphidium advenum											1						
Elphidium cuvillieri													2	1	3		
Elphidium oceanensis												1					
Elphidium williamsoni						1	2	1	1		6	9			1		
Entzia macrescens		151	82	94	181	97	101	121	72	26		1					
Fissurina lucida											26	3	1				
Glomospira gordialis				1	1	2	6	5	2								
Haplophragmoides manilaensis							1		1								
Haynesina depressula									41	16	75	129	86	3	40	4	2
Haynesina germanica								2		4	21	11	2		5	3	
Helenina anderseni						4	16	48	24	26	1						
Lepidodeuterammina ochracea											1						
Leptohalysis scotti															2		
Miliammina fusca		3	18	20	6	45						5	1				1
Morulaeplecta bulbosa														3			
Quinqueloculina bosciana		10	60	19		6	4	3	3	12	3	6	5				
Quinqueloculina laevigata													9			1	
Quinqueloculina lata												1					
Quinqueloculina pseudobuchiana			1	2									5			2	
Quinqueloculina seminulum			1					3	2	3	1		5			1	
Reophax moniliformis											3	5	2	1		1	
Reophax nana															1	1	1
Siphotrochammina lobata				4			2	18	2								
Textularia earlandi													1	1			
Trichohyalus aguayoi		2	23	5			1	3	1	3							
Triloculina oblonga				1													
Trochammina inflata		13	43	17	44	61	86	33	73	27	1	1					
others				2													
Total		201	264	183	233	227	232	248	284	215	160	223	168	16	77	53	18
Species no., counted		7	9	14	5	10	10	15	14	16	18	21	20	8	11	12	10
Volume (cm^3)		7	10	10	10	13	15	15	13	15	13	14	13	10	11.5	15	12
Split (n)		1	0.03	0.06	0.25	0.5	0.5	0.63	0.25	0.56	1	1	1	1	1	1	1
Population density (ind./10 cm^3)		287	8448	2928	932	349	309	265	874	255	123	159	129	16	67	35	15
Fisher alpha index		1.4	1.8	3.5	0.9	2.1	2.4	3.5	3.1	4.0	5.2	5.7	5.9	6.4	3.5	4.8	9.3

Supplement Table 6. Foraminiferal census data 2019, Ria Formosa salt marsh transect.

Sampling date: 6-May-2019															
Counted specimens Sample:	207	208	209	210	211	212	213	214	215	216	217	218	219	220	221
Section m:	3.0	7.0	15.0	22.0	25.0	29.0	37.0	48.0	52.0	56.0	61.5	72.6	81.0	87.1	89.0
Species Hight (m POD):	1.48	1.37	1.27	1.20	1.21	0.93	0.81	0.52	0.31	0.18	0.09	-0.10	-0.24	-0.34	-0.46
Affinetrina planciana		48	1		2		4		9	11					
Ammonia aberdoveyensis	43	31	7	9	2		32	33							
Ammonia advena								1							
Ammonia tepida							1		10	8	3	7	3	5	3
Ammoscalaria runiana				1		1	1				1	3	8	6	3
Ammotium salsum					1	1		19							
Arenoparrella mexicana								2							
Aubignyna hamblensis									4	4	7	4	5	4	
Bisaccium imbricatum									1				3		
Bolivina italica											1				1
Bolivina ordinaria												1		1	
Bolivina striatula										4	3	2	1	1	1
Buccella granulata										2			2		
Buliminella elegantissima														1	3
Cornuspira involvens					1		1				1	2			
Crithionina mamilla										2			1		
Eggerella europea						1	3								
Eggerelloides scaber															1
Elphidium advenum									4	1	1				
Elphidium cuvillieri									1	4	1	4	4	36	2
Elphidium oceanensis									1	1					
Elphidium williamsoni				2		1	6	1	33	25	9		2	1	
Entzia macrescens	40	52	229	94	145	62	38	38		1			1		
Fissurina lucida		1							11	9			1	10	
Glomospira gordialis		3	6	1	4	4	2								
Haynesina depressula				30		26	62		170	106	256	28	50	58	4
Haynesina germanica			1			1	1		32	14	7	2	3		
Helenina anderseni				1	5	7	22	56							
Lepidodeuterammina ochracea														1	
Miliammina fusca	1	1	76	3				1			1	4	4	1	
Miliolinella hybrida														2	
Morulaeplecta bulbosa													1	5	
Neoconorbina terquemi														1	
Quinqueloculina bosciana	9	21	6	9	16	4	3	76	1	10	9	2	2	6	
Quinqueloculina laevigata		1						1			3	1		9	4
Quinqueloculina lata										2			1		
Quinqueloculina limbata															1
Quinqueloculina parvula															1
Quinqueloculina pseudobuchiana				2						13	3		1	3	4
Quinqueloculina seminulum	1	6				1	3	1	8	7	4	5	4		9
Reophax arctica														8	
Reophax moniliformis								1	2	1	1	3	3	3	
Reophax nana												2	2		
Siphotrochammina lobata			1		1	6		1							
Textularia earlandi													1	3	
Trichohyalus aguayoi	27	9					3								
Triloculina oblonga								2	1						
Trochammina inflata	33	20	35	12	54	45	31	54						1	
sonstige										2			1	4	
Total	154	193	362	164	231	160	213	287	288	227	311	70	104	170	37
Species no., counted	7	11	9	11	10	13	16	15	15	20	17	15	23	24	13
Volume (cm^3)	10	10	9	10	16	15	14	17	15	13	14	14	11.5	12.5	9
Split (n)	0.03	0.06	0.25	0.06	0.25	0.13	0.25	1	0.5	0.13	0.25	1	1	1	1
Population density (ind./10 cm^3)	4928	3088	1609	2624	578	853	609	169	384	1397	889	50	90	136	41
Fisher alpha index	1.5	2.5	1.7	2.7	2.1	3.3	4.0	3.4	3.4	5.3	3.9	5.9	9.1	7.6	7.1

Supplement Table 7. Faunal and environmental parameters, Ria Formosa salt marsh transect.

Year	Sample	Section m	Textulariida (%)	Miliolida (%)	Rotaliida (%)	*Ammonia* dissolution index	Innundation time (%)	pCO_2 (µatm)	Ω Ca	Corg (%)
2018	190	0	83.1	5.5	11.4		1.8			0.4
	191	3	54.2	24.2	21.6	1.6	3.8	6455	0.70	
	192	7	74.9	15.3	8.7	1.4	6.4	10187	0.44	1.6
	193	15	100.0	0.0	0.0		9.5	29826	0.19	10.9
	194	22	91.2	2.6	6.2	2.6	11.1	32918	0.12	11.3
	195	25	84.5	1.7	13.8	3.3	11.1	33919	0.13	
	196	29	72.6	3.2	24.2	2.8	20.2	21274	0.21	5.6
	197	37	53.5	2.8	43.7	2.5	26.9	47875	0.06	5.0
	198	48	26.0	14.9	59.1	2.0	41.2	29389	0.16	1.6
	199	52.2	3.8	5.0	91.3	2.0	55.5	2061	1.66	
	200	56.1	10.8	6.7	82.5	2.3		6336	0.59	0.5
	201	61.5	4.8	16.7	78.6	2.3		2412	1.50	
	202	72.6	56.3	0.0	43.8			8014	0.52	
	203	81	3.9	0.0	96.1					2.3
	204	87.1	20.8	7.5	71.7					0.7
	205	89	44.4	0.0	55.6					0.3
2019	207	3	48.1	6.5	45.5	1.7	3.8	3988	0.80	17.1
	208	7	39.4	39.4	21.2	1.6	6.2	4378	0.70	14.0
	209	15	95.9	1.9	2.2	3.6	8.8	22285	0.68	11.8
	210	22	67.7	6.7	25.6	2.8	11.1	23132	0.15	7.9
	210 (rept)	22						60588	0.07	
	211	25	88.7	8.2	3.0	4.0	10.8	20522	0.14	2.1
	212	29	75.0	3.1	21.9		21	9038	0.29	6.0
	213	37	35.2	5.2	59.6	3.5	26.5	13624	0.22	6.2
	214	48	40.4	27.9	31.7	3.4	42.3	17663	0.19	0.9
	215	52	0.7	6.6	92.7	2.3	52.2	8846	0.36	0.4
	216	56	1.8	18.9	78.4	2.3		3232	0.90	0.8
	217	61.5	1.0	6.4	92.6	2.0		5269	0.57	1.2
	218	72.6	17.1	14.3	68.6	2.4		7776	0.34	1.3
	219	81	20.2	7.7	71.2	2.3		4625	0.58	2.3
	220	87.1	16.5	11.8	69.4	1.8		1982	1.37	1.8
	221	89	10.8	51.4	37.8					0.8

Year	Sample	Section m	Stage 1	Stage 2	Stage 3	Stage 4	Stage 5	Total	Dissolution index (weighed mean)
2018	191	3	15	19				34	1.6
	192	7	7	4				11	1.4
	194	22		4	3	1		8	2.6
	195	25		2	5	6		13	3.3
	196	29		1	4			5	2.8
	197	37		34	16	7		57	2.5
	198	48	18	8	18			44	2.0
	199	52.2	3	1	3			7	2.0
	200	56.1		9	4			13	2.3
	201	61.5	2	4	3	1		10	2.3
2019	207	3	22	13	8			43	1.7
	208	7	20	4	7			31	1.6
	209	15		2		4	1	7	3.6
	210	22		3	5	1		9	2.8
	211	25				2		2	4.0
	213	37		4	10	17	1	32	3.5
	214	48		6	10	14	3	33	3.4
	215	52	4		5	1		10	2.3
	216	56	2	2	4			8	2.3
	217	61.5		3				3	2.0
	218	72.6		5	1	1		7	2.4
	219	81		2	1			3	2.3
	220	87.1	3		2			5	1.8

Ammonia spp. preservation stages
Stage 1: shell glossy and intact
Stage 2: dull or opaque chamber walls
Stage 3: dissolution or loss of final chamber wall
Stage 4: dissulution of the walls of two or more chambers, IOL visible
Stage 5: star-shaped test, only the IOL is left on the outer chamber walls